Forest Ecology and Management 438 (2019) 267–284

Contents lists available at ScienceDirect

Forest Ecology and Management

journal homepage: www.elsevier.com/locate/foreco

Wood quality attribute models and their utility when integrated into density management decision-support systems for boreal conifers

P.F. Newton

Canadian Wood Fibre Centre, Canadian Forest Service, Natural Resources Canada, 1219 Queen Street, Sault Ste. Marie, Ontario P6A 2E5, Canada

ARTICLE INFO

Keywords:
Commercially-relevant fibre attributes
Hierarchical mixed-effects models
Structural stand density management models
Jack pine
Black spruce

ABSTRACT

The objectives of this study were to (1) develop wood quality prediction models for a suite of commercially-relevant jack pine (*Pinus banksiana* Lamb.) fibre attributes (wood density (W_d), microfibril angle (M_a), modulus of elasticity (M_e), fibre coarseness (C_o), tracheid wall thickness (W_t), tracheid radial (D_r) and tangential (D_t) diameters and specific surface area (S_a)), (2) given (1), incorporate the parameterized equations within structural stand density management models (SSDMMs), and (3) given (2), exemplify their utility in silvicultural decision-making via the comparative assessment of attribute outcomes arising from operationally-relevant crop plans. Analytically, the equations were developed deploying Silviscan-determined attributes derived from transverse breast-height radial xylem sequences obtained from 61 trees sampled from 2 geographically-separated thinning experiments located in the central region of the Canadian Boreal Forest Region. Hierarchical mixed-effects regression modeling combined with cross-validation procedures were used to specify, parameterize and evaluate the attribute-specific prediction equations. Overall, the results revealed that the attribute trajectories were size-dependent and the resultant models were adequate in terms of their goodness-of-fit characteristics (e.g., I^2 values of 75, 71, 71, 66, 60, 55, 49 and 38% for C_o, M_e, W_t, S_a, W_d, M_a, D_r and D_t respectively), lack-of-fit indicators (e.g., temporally invariant patterns of absolute and relative errors devoid of evidence of systematic bias), and predictive performance (e.g., 95% probability that 95% of all future relative D_t, D_r, S_a, W_d, C_o, W_t, M_e and M_a errors would be within ± 5, ± 9, ± 11, ± 12, ± 12, ± 13, ± 35 and ± 43% of their true values, respectively). Incorporating the jack pine equations along with a similar suite of functions previously developed for black spruce (*Picea mariana* (Mill) B.S.P) into the SSDMM analytical framework, yielded a pair of enhanced stand-type-specific (natural-origin and planted stands) decision-support systems for each species. These systems enabled the estimation of attribute-specific developmental trajectories for the rotational tree population from which diameter-class and stand-level wood quality performance measures were derived. As exemplified, the development of size-dependent fibre attribute prediction models and their subsequent integration within SSDMMs provides forest managers with a decision-support platform for evaluating and comparing end-product-related consequences of selected crop plans.

1. Introduction

Jack pine (*Pinus banksiana* (Mill) B.S.P.) is an intensively-managed coniferous species which occupies a wide range of sandy site types throughout the Canadian Boreal Forest Region (Rowe, 1972). The species is a major feedstock for numerous conversion mills that derive a multitude of commercially-relevant end-products from harvested logs including dimensional lumber and associated solid wood derivatives (window frames, doors, shelving, mouldings and panelling), composite building materials (glulam-based beams, headers, and trusses, and finger-jointed joists and rafters), and pulp and paper products (paperboards, newsprint, facial tissues and specialized coated papers) (Zhang and Koubaa, 2008). The end-product potential of an individual jack pine tree is largely governed by the (1) internal wood quality characteristics of the xylem tissue (e.g., wood density, microfibril angle, modulus of elasticity, tracheid wall thickness, fibre coarseness, radial and tangential tracheid diameters, and specific surface area), and (2) external morphological characteristics (e.g., stem size (diameter, height), taper, sweep and branchiness). Functionally, the internal attributes can be explicitly linked to various performance measures which are used to define the overall type and grade of potential end-products (Defo, 2008). For example, the stiffness and strength of extracted solid wood products such as dimensional lumber are directly proportional to modulus of elasticity and wood density, respectively, and inversely

E-mail address: peter.newton@canada.ca.

https://doi.org/10.1016/j.foreco.2019.01.053
Received 1 November 2018; Received in revised form 28 January 2019; Accepted 30 January 2019
Available online 04 March 2019

proportional to microfibril angle. Similarly, the tear and tensile strength of extracted paper products are directly proportional to fibre coarseness and specific surface area, respectively.

Quantitatively, the cumulative temporal developmental trends of fibre attributes within commercially-important boreal conifers has been characterized as polymorphic-like and size-dependent (e.g., black spruce (*Picea mariana* (Mill.) B.S.P.); Newton, 2016). These fibre attribute development trajectories can be manipulated through various stand-level forest management inputs and by consequence affect end-product outcomes (sensu Barbour et al., 2003). These inputs included crop planning decisions such as species, genotype and initial spacing (IS) choices at the time of establishment, and the timing and intensity of subsequent density management treatments (precommercial thinning (PCT) and commercial thinning (CT)) applied over the rotation (Kang et al., 2004; Watt et al., 2011; Rais et al., 2014). Currently, explicitly managing for end-products by controlling fibre attribute developmental patterns is challenging given the general lack of crop planning decision-support tools that include fibre prediction models that are capable of producing wood quality outcome metrics (sensu Defo et al., 2016).

Analytically, however, the size-dependency of attribute developmental trajectories provides a plausible mechanism for embedding attribute prediction equations within crop planning decision-support systems that include diameter distribution recovery modules. The structural stand density management model (SSDMM) which has been developed for a number of boreal species (e.g., jack pine, black spruce and mixed jack pine – black spruce stand-types (Newton, 2009, 2012a, 2012b, 2012c)), is one such system that includes the prerequisite functionality. Specifically, SSDMMs employ Weibull-based parameter prediction equations to recover the diameter distribution at any point during a stand's development. This functionality enables the potential integration of size-dependent fibre attribute prediction equations which could generate the required wood quality metrics for evaluating end-product potentials of specified crop plans. Contextually, SSDMMs are classified as stand-level distance-independent size distribution yield projection systems (sensu Porté and Barlelink, 2002) which are comprised of an integrated set of functional and empirical relationships that collectively quantifies the effects of density management on stand development. These relationships include the reciprocal equations of the competition–density (C-D) and yield–density (Y-D) effect (Kira et al., 1953; Shinozaki and Kira, 1956), self-thinning rule (Yoda et al., 1963; Newton, 2006), composite height-diameter, taper, biomass, product and value equations (e.g., Newton and Amponsah, 2007), diameter recovery parameter prediction equation systems (e.g., Newton and Amponsah, 2005), and response models for quantifying genetic worth and thinning effects (Newton, 2015a, 2015b, respectively). Furthermore, as empirically validated, the predicted stand structure developmental patterns and associated yield outcomes produced from these SSDMMs, largely conform to expectation in regards to known forest dynamic processes and ecological axioms (see Newton (2015c) for a comprehensive assessment).

SSDMMs produce a comprehensive set of outcome metrics which are useful in designing density management regimes for a given stand-level management objective. These include annual, periodic and rotational performance metrics reflective of volumetric productivity (e.g., piece-size), product production (e.g., mill-type-specific (stud and randomized length) chip and lumber volumes), and economic viability (e.g., land expectation value given inputted fixed and variable cost assumptions). Currently, however, SSDMMs lacks the ability to predict commercially-relevant fibre attributes which underlie end-product potential. Consequently, the goal of this study was to examine the plausibility of developing and integrating fibre attribute prediction models into the SSDMM platform. Analytically, this goal was addressed by realizing the following 3 sequential objectives. Firstly, developing size-dependent hierarchical mixed-effects regression equations for a suite of commercially-relevant fibre attributes that underlie end-product type and grade: wood density, microfibril angle, modulus of elasticity, fibre coarseness, tracheid wall thickness, tracheid radial diameter, tracheid tangential diameter and specific surface area (henceforth denoted W_d, M_a, M_e, C_o, W_t, D_r, D_t and S_a, respectively). Secondly, incorporating the resultant functions along with a previous developed equation suite for black spruce (Newton, 2016), into the species-specific SSDMMs developed for natural-origin and plantation stand-types (Newton, 2009, 2012a). Thirdly, demonstrating the utility of the enhanced SSDMMs in silvicultural decision-making via the comparative assessment of fibre attribute outcomes arising from operationally-relevant crop plans.

2. Material and methods

2.1. Development of hierarchical mixed-effects fibre attribute prediction equations

2.1.1. Data acquisition, disk processing and fibre attribute determination

Sixty-one trees from two geographically-separated (450 km) long-term (monitored for 20 + years) jack pine thinning experiments located in the north-eastern (denoted the Sewell site which falls within the Sewell River watershed) and north-central (denoted the Tyrol site which falls within the western portion of the Namewaminkan River watershed) regions of the Canadian Province of Ontario, were selected for analyses. These trees were grown under a nominal range of silvicultural intensities for natural-origin stand-types which are reflective of the forest management strategies currently employed in the central portion of the Canadian Boreal Forest Region (McKinnon et al., 2006). Specifically, these included an (1) extensive regime in which no density management treatments were implemented, (2) low intensive regime involving the early application of PCT treatments in order to shorten the time to stand operability status, and (3) moderate intensive regime involving both PCT and CT treatments in order to capture merchantable volume mortality losses and diversify end-product potential at rotation. At the Sewell site, 31 jack pine sample trees were selected within 6 variable-size plots that were established in 3 jack pine stands that had regenerated naturally following a stand-replacing wildfire event during the 1958–1960 period. The sample trees were selected deploying a pseudo-stratified random sampling design in which trees were choosen across the observed diameter distribution (e.g., approximately 1 tree was selected within each diameter-class-based quintile). The sample trees were devoid of visible deformities such as major stem forks, periderm injuries (blazing scars), and damaged crowns. The stands were situated on medium-to-good quality sites (mean site index of 18 m@50 yr; Carmean et al., 2001), geographically located within Forest Section B.7 – Missinaibi-Cabonga of the Canadian Boreal Forest Region (Rowe, 1972), and were approximately 53 years of age at breast height (1.3 m) when sampled in 2013. The glacial-derived soils were characterized as deep (> 1 m) with coarse-to-medium sandy textures situated on gently undulating (rolling) topography. Silviculturally, the stands were subjected to 1 of 3 treatments, resulting in 3 different density management regimes: (1) unthinned controls; (2) PCT at age 11 (1971); and (3) PCT at age 11 followed by a light pseudo-CT at age 43 (2003).

At the Tyrol site, 30 jack pine sample trees were selected within 4 variable-size plots that were established in 2 jack pine stands which had regenerated naturally following a stand-replacing wildfire event during the early 1940s. Similar to the Sewell site, the sample trees were devoid of visible deformities and selected deploying a pseudo-stratified random sampling design. The Tyrol stands were situated on good-to-excellent quality sites (mean site index of 21 m@50 yr; Carmean et al., 2001), geographically located within Forest Section B9 (Superior) of the Canadian Boreal Forest Region (Rowe, 1972), and were approximately 71 years of age at breast height when sampled in 2015. Similar to the Sewell site, the soils were characterized as deep (> 1 m) with fine sandy textures situated on gently rolling topography. These stands were subjected to 2 density manipulation treatments: PCT at age 18 (1962) followed a light pseudo-CT treatment during 1998 at an age of

Table 1
Descriptive statistical summary of the mensurational characteristics and breast-height wood quality fibre attributes of the 61 jack pine sample trees.

Variable	Unit	Mean	Standard error	Minimum	Maximum	Coefficient of variation (%)
Diameter at breast-height (1.3 m)	cm	20.5	2.93	14.7	27.0	14.3
Age at breast-height	yr	59	9	47	71	15.8
Wood density	kg/m^3	438.0	31.04	358.1	509.4	7.1
Microfibril angle	°	13.9	2.90	8.1	20.7	20.9
Modulus of elasticity	GPa	12.5	1.87	8.3	16.3	14.9
Fibre coarseness	µg/m	412.1	27.91	366.4	481.9	6.8
Tracheid wall thickness	µm	2.8	0.22	2.2	3.3	8.0
Tracheid radial diameter	µm	30.8	1.22	28.3	33.5	4.0
Tracheid tangential diameter	µm	27.7	0.68	26.2	29.7	2.5
Specific surface area	m^2/kg	308.7	20.43	263.9	355.3	6.6

approximately 54. In summary, the 61 sample trees selected were representative of the diameter-class range observed at the time of sampling and hence were considered an appropriate sample population for examining size-dependent differences in fibre attribute developmental patterns. Table 1 includes a descriptive statistical summary of the mensurational characteristics of the sample trees.

In terms of field sampling, at the conclusion of the 2013 and 2015 vegetative growing seasons at the Sewell and Tyrol sites, respectively, each selected sample tree was felled and sectioned deploying destructive stem analysis. Specifically, each sample tree was felled at stump height (≈0.3 m), delimbed and topped at an 80% relative height position. The stem was then sectioned into 0–20%, 20–40%, 40–60% and 60–80% log-length intervals employing a percent-height sampling protocol. Cross-sectional samples were extracted at stump height (0.3 m), breast-height (1.3 m), relative height positions of 10, 30, 50 and 70% (centre-point of each of the 4 logs), and at the 80% relative height position, yielding a total of 7 disks per tree. These disks were immediately (≤8 h) placed in short-term cold storage (< 0 °C) near the sampling sites, subsequently transported and placed in long-term cold storage (< 0 °C) at the Great Lakes Forestry Centre (Sault Ste. Marie, Ontario, Canada), and eventually shipped to FPInnovations (Vancouver, British Columbia, Canada) for laboratory processing and fibre attribute determination deploying the Silviscan-3 system. Note, for the purposes of this study, only the results for the breast-height disk were utilized. Briefly, the Silviscan-3 system is the most recent variant of the Silviscan system originally developed by CSIRO's (Commonwealth Scientific and Industrial Research Organisation) Forestry and Forest Products Division, in Australia. Automated image acquisition and analysis (cell scanner), X-ray densitometry, and X-ray diffractometry, are combined into an integrated system from which a multitude of commercially-relevant xylem attributes can be readily determined. These include radial and tangential tracheid diameters, and tracheid wall thickness as directly determined from image analysis (Evans, 1994), wood density as directly derived from X-ray densitometry (Evans, 1994), microfibril angle as directly ascertained through X-ray diffraction (Evans et al., 1996), and the modulus of elasticity as indirectly determined via a combination of X-ray densitometry and diffraction measurements (Evans, 2006). Fibre coarseness and specific surface area are indirectly calculated using the cell dimensions and wood density estimates (Evans, 1994). The preparatory laboratory-based processing involved the extraction of a 2 × 2 cm transverse bark-to-pith-to-bark sample along the geometric mean diameter of each breast-height cross-sectional disk. One of the two pith-to-bark radial sequences was randomly selected from each of the 61 transverse samples. These sequences were then subjected to extraction techniques so that resins that could influence density estimates were removed prior to the Silviscan-3 analysis. This consisted of soaking the samples in acetone for 12 h followed by extraction for 8 h at 70 °C using a modified Soxhlet system. The sequences were then air-dried for approximately 12 h, conditioned to a 40% relative humidity at a temperature of 20 °C, and then processed via the Silviscan-3 system. A descriptive statistical summary of the resultant attribute estimates is provided in Table 1.

2.1.2. Computations and analyses

In order to control for intrinsic physiological-based age-dependent effects on fibre attribute development among a group of sample trees that differed in their chronological breast-height ages due to differential rates of height growth during early stand-development, cambial age (number of annual rings from the pith) was employed as the temporal variate of change in the first-level hierarchical model specification (level-one independent variable). The corresponding fibre attribute value (level-one dependent variable) was represented by the pith-to-bark cumulative annual ring-area-weighted moving average (Eq. (1)).

$$V_{(li)(k)} = \frac{\sum_{j=1}^{i} v_{(lj)(k)}\, a_{lj}}{\sum_{j=1}^{i} a_{lj}} \tag{1}$$

where $V_{(li)(k)}$ is the cumulative annual ring-area-weighted moving average specific to the kth attribute (wood density, microfibril angle, modulus of elasticity, fibre coarseness, tracheid wall thickness, tracheid radial diameter, tracheid tangential diameter or specific surface area) and lth sample tree calculated from cambial age 1 up to the ith cambial age, $v_{(lj)(k)}$ is the mean annual area-weighed value specific to the kth attribute, lth sample tree and jth annual ring, and a_{lj} is the area of the jth annual ring (mm^2) specific to the lth sample tree. Note, the $V_{(li)(k)}$ value for a given tree reflects the accumulated status of the kth attribute up to the ith cambial age and hence can be used to indirectly infer the composite end-product potential of a tree if it was harvested at that specific age.

2.1.3. Model specification, parameterization and evaluation

2.1.3.1. Specification. Preliminary graphical analysis was used to examine the temporal trends of each individual-tree attribute-specific time series and their relationship with tree size (diameter). This analysis indicated that the attribute-specific polymorphic-like nonlinear relationships varied systematically with tree size (Fig. 1). Consequently, at the first hierarchical level, an exponential-based specification was selected to describe these trends (sensu Ratkowsky, 1990): specifically, the modified Hoerl's (1954) compound exponential function (Eq. (2)).

$$V_{(li)(k)} = \alpha_{0l_{(k)}} a_{c(li)}^{\alpha_{1l_{(k)}}} e^{\alpha_{2l_{(k)}} a_{c(li)} + \alpha_{3l_{(k)}} a_{c(li)}^2} \varepsilon_{(li)(k)} \tag{2}$$

where $\alpha_{ml_{(k)}}$, $m = 0,..,3$ are model parameters specific to the kth attribute and lth sample tree, $a_{c(li)}$ is the ith cambial age specific to the lth sample tree, and $\varepsilon_{(li)_{(k)}}$ is a random error term specific to kth attribute, lth sample tree and ith cambial age. The Hoerl's function has shown promise in describing complex nonlinear patterns as exemplified by Daniel and Wood (1980). In relation to wood quality modelling, Newton (2016) demonstrated its specific utility in describing the fibre attribute developmental trends of black spruce. Nevertheless, in this study, the specific applicability of the modified Hoerl model for jack

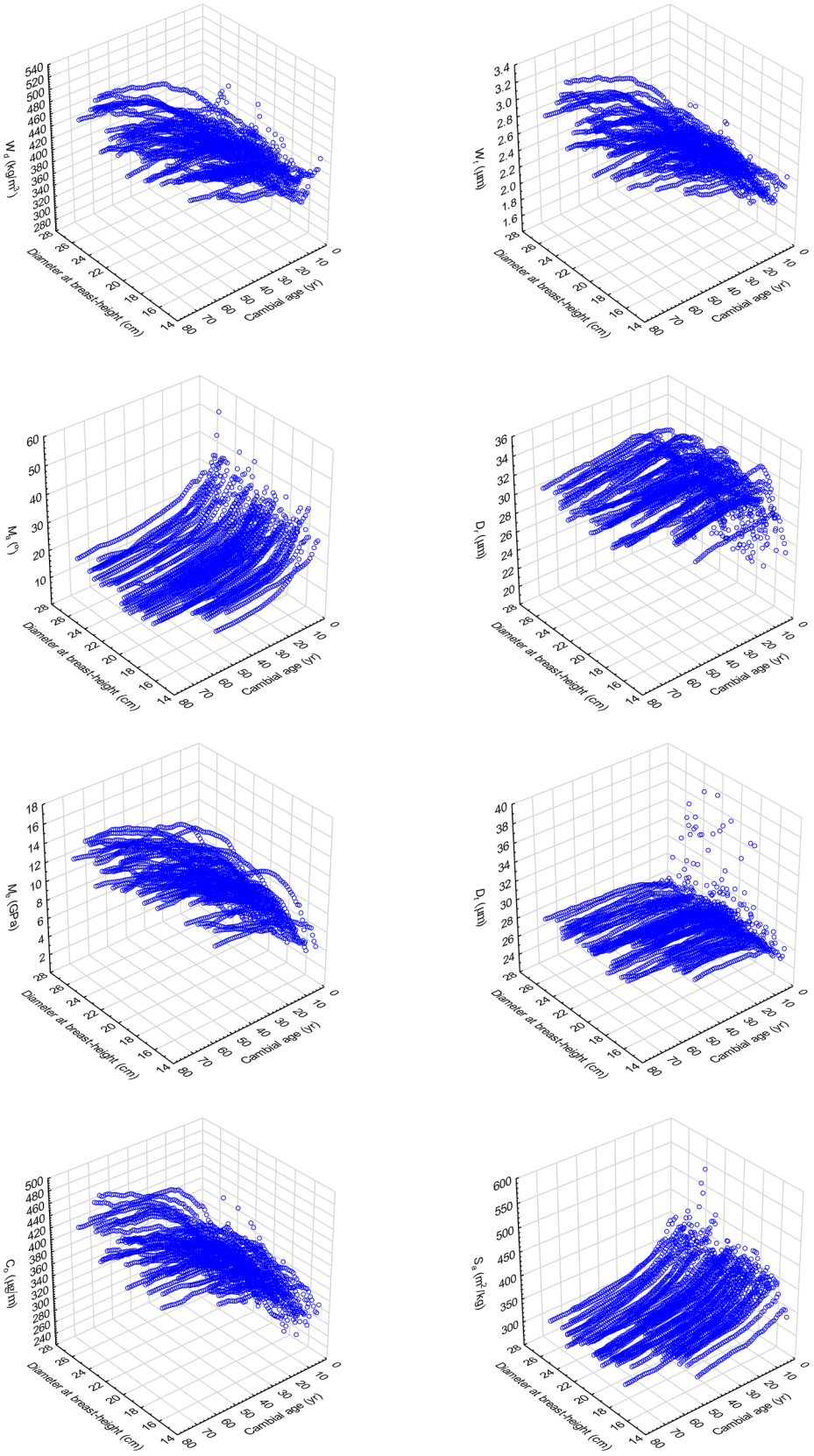

Fig. 1. Three-dimensional visualization of tree-specific temporal developmental trends graphically illustrating patterns of change in attribute-specific cumulative area-weighted moving average values with increasing cambial age and tree size.

pine was assessed directly. Each individual tree-based attribute-specific temporal trajectory was fitted with the logarithmically-transformed variant of the full model (Eq. (2)), along with a logarithmically-transformed reduced model variant in which the exponential square term was excluded. The resultant models were then compared to determine the statistical significance of including the squared term

(sensu Gujarati, 2006). This comparative analysis supported the selection of the modified Hoerl-based variant as the most applicable first-level model specification: i.e., the squared term was significant ($p \leq 0.05$) in 79, 85, 75, 95, 93, 74, 100 and 94% of the W_d, M_a, M_e, C_o, W_t, D_r, D_t and S_a individual-tree regressions, respectively.

The size-dependence of the individual-tree attribute-specific trajectories was revealed graphically via an examination of the 3D-scatterplots (Fig. 1), and statistically through correlation analyses. The latter analysis consisted of firstly obtaining ordinary least squares parameter estimates for the logarithmically-transformed modified Hoerl model by attribute for each tree. Secondly, the magnitude and significance of the correlation coefficient for the relationship between each of the 4 parameters and cumulative tree size (diameter at breast-height (d_b) at the time of sampling) was determined and assessed. These results largely confirmed the graphical-based size-dependent inference: i.e., at least 1 of the 4 coefficients were linearly correlated ($p \leq 0.10$) with diameter for 6 of the 8 attributes assessed (W_d, M_e, C_o, D_r, D_t and S_a).

Analytically, the hierarchical mixed-effects regression model was then derived as follows: (1) re-expressing the 1st level hierarchical model specification into its logarithmic equivalent (Eq. (3)), (2) specifying the 2nd level models in which the first-level parameters were expressed as linear functions of cumulative tree size (Eq. (4)), and (3) given (1) and (2), re-incorporating the 2nd level models back into the logarithmic variant of the 1st level model resulting in the final hierarchical model specification (Eq. (5)).

$$\log_e(V_{(li)(k)}) = \log_e \pi_{0l_{(k)}} + \pi_{1l_{(k)}} \log_e(a_{c(li)}) + \pi_{2l_{(k)}} a_{c(li)} + \pi_{3l_{(k)}} a^2_{c(li)} + \log \varepsilon_{(li)(k)} \quad (3)$$

where $\pi_{ml_{(k)}}$, $m = 0,1,2,3$ are size-dependent 1st level change parameters specific to the kth attribute which are allowed to vary randomly across sample trees, and $\log \varepsilon_{(li)(k)}$ is a random error at the ith cambial age for the lth sample tree specific to the kth attribute, that is assumed to be normally distributed with a mean of zero, and uncorrelated across sample trees.

$$\pi_{ml_{(k)}} = \beta_{m0_{(k)}} + \beta_{m1_{(k)}} d_{b(l)} + U_{ml_{(k)}} \text{ where } m = 0, 1, 2, 3 \quad (4)$$

where $\beta_{mn_{(k)}}$, $n = 0,1$ are second-level parameters specific to the kth attribute which represents the effect of tree size (d_b) on the mth level-one parameter, and $U_{ml_{(k)}}$ is the second-level random effect error term specific to the mth parameter, lth sample tree and kth attribute.

$$\begin{aligned}\log_e(V_{(li)(k)}) = {} & \beta_{00_{(k)}} + \beta_{01_{(k)}} d_{b(l)} + \beta_{10_{(k)}} \log_e(a_{c(li)}) + \beta_{11_{(k)}} d_{b(l)} \log_e(a_{c(li)}) \\ & + \beta_{20_{(k)}} a_{c(li)} + \beta_{21_{(k)}} d_{b(l)} a_{c(li)} + \beta_{30_{(k)}} a^2_{c(li)} + \beta_{31_{(k)}} d_{b(l)} a^2_{c(li)} \\ & + U_{0l_{(k)}} + U_{1l_{(k)}} \log_e(a_{c(li)}) + U_{2l_{(k)}} a_{c(li)} + U_{3l_{(k)}} a^2_{c(li)} + \log_e(\varepsilon_{(li)(k)})\end{aligned} \quad (5)$$

where $\beta_{i'j'(k)}$, $i' = 0, 1, 2, 3$ and $j' = 0,1$ are model parameters specific to the kth attribute.

2.1.3.2. Parameterization. Statistically, serial correlation may be present within fibre attribute developmental sequences composed of cumulative moving average values (e.g., Newton, 2016). Consequently, partial autocorrelation coefficients were deployed to determine the presence of serial correlation within each attribute sequence for each sample tree. Resultantly, significant ($p \leq 0.05$) first-order serial correlation between adjacent consecutive values was found to be present in all sequences irrespective of attribute. Furthermore, significant ($p \leq 0.05$) second-order serial correlation was also occasionally present. Thus to potentially avoid erroneous model specification and associated inferences regarding the importance of the potential covariates and the significance of the parameter estimates due to the presence of serial correlation, each individual-tree attribute-specific sequence was reduced. The degree of reduction was determined by systematically removing consecutive values at various temporal lags until the presence of significant serial correlation was eliminated. The results of this preliminary assessment indicated that partial autocorrelation coefficients were largely non-significant ($p < 0.05$) when 2 or more consecutive values were removed. Consequently, a data stratification procedure in which consecutive values were removed in a systematic fashion was implemented. Starting from the 2nd cambial year, this involved removing values for 3rd and 4th cambial years, 6th and 7th cambial ages, and so on, for each sequence. This ultimately resulted in the creation of calibration and validation data subsets consisting of retained and removed observations, respectively. Additionally, in order to potentially account for stand-type or density management regime effects, the attribute values for the thinning treatment years were also retained within the calibration data subset: i.e., attribute values for the years 1971 and 2001 for the trees sampled at the Sewell site, and the years 1962 and 1998 for the trees sampled at the Tyrol site. In summary, this stratification procedure resulted in a calibration data subset consisting of 1232 observations per attribute (i.e., comprised of attribute values for cambial ages 2,5,8,11,…,$n-1$ inclusive of ages at which thinning treatments were implemented), and a validation data subset consisting of 2271 observations per attribute (i.e., comprised of attribute values for cambial ages 3,4,6,7,..,n).

The hierarchical linear and nonlinear modeling software program, HLM7 (Raudenbush et al., 2011), was used to derived parameter estimates for each attribute-specific model (Eq. (5)) deploying the calibration data subset. Statistically, the program provides empirical Bayes estimates for the 1st level coefficients, generalized least squares estimates for the 2nd level coefficients, and maximum-likelihood estimates for the variance and covariance components (sensu Raudenbush et al., 2011). The parameter estimates from the 1st level regression relationships were treated as random whereas the parameter estimates from the 2nd level relationships were treated as fixed. However, upon parameterization it was evident that convergence would not be obtained unless the parameter for the square term ($\pi_{3l_{(k)}}$) was treated as fixed. Consequently, the model specification was adjusted accordingly, re-parameterized and subsequently evaluated on the significance of the fixed effects (d_b) deploying both univariate and multivariate tests of significance. Analogous to the backward variable selection method commonly used in stepwise regression analysis (Neter et al., 1990), the specification process continued by removing insignificant size-dependent terms ($p > 0.05$) in an iterative fashion until the reduced model specifications only consisted of variables that were significantly ($p \leq 0.05$) contributing to explaining the variation of a given dependent variable.

These final model forms were then evaluated for compliance to the underlying statistical assumptions according to the protocol advanced by Raudenbush and Bryk (2002). These included (1) assessing the constant variance assumption using the test statistic for homogeneity, (2) determining the presence of significant size-dependent fixed effects using multivariate contrasts, (3) validating the final model specification by determining if other 2nd level covariates should have been explicitly included (e.g., testing to determine if thinning significantly influenced the 1st level parameters using an indicator variable), and assessing the significance of the random effect terms (i.e., testing the null hypothesis that the level-one parameters included random variation among individual trees versus the alternative hypothesis of no random variation). Using raw residual scatterplots, the parameterized models were also assessed for the presence of potential outliers, influential observations and systematic biases. The occurrence of serial correlation among the first-level Bayes residuals within an individual-tree attribute sequence was evaluated deploying an autocorrelation coefficient in conjunction with the Box-Ljung statistic. The proportion of variation explained by the regression models in their untransformed specification and associated observed-predicted scatterplots, were also used to assess overall model performance.

2.1.3.3. Model evaluation: goodness-of-fit, lack-of-fit, and predictive ability. Employing the validation data subset, the retransformed

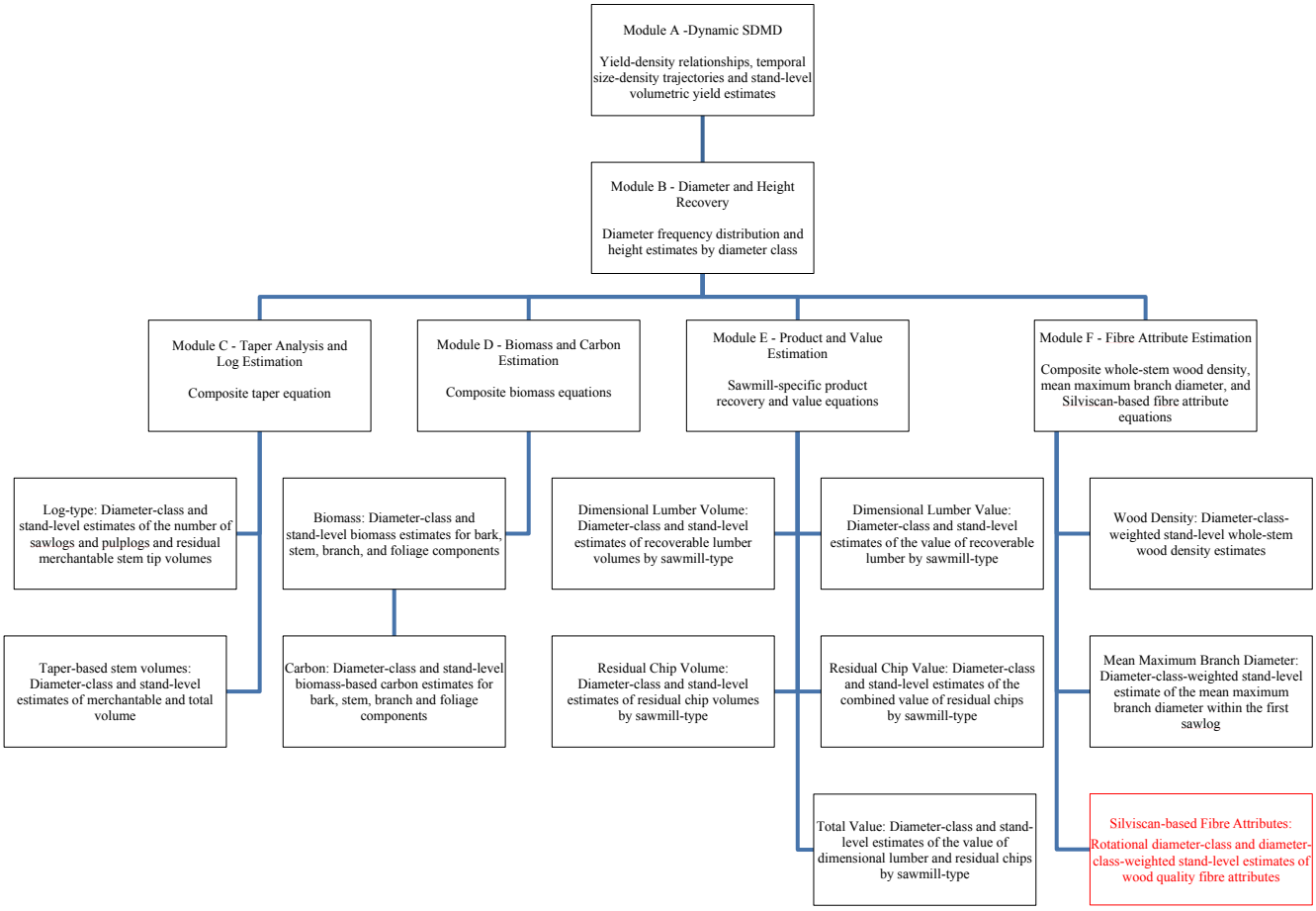

Fig. 2. Schematic illustration of the enhanced modular-based structural stand density management model with the inclusion of the new Silviscan-based fibre attribute prediction sub-module (denoted in red). (For interpretation of the references to colour in this figure legend, the reader is referred to the web version of this article.)

parameterized models were assessed using goodness-of-fit, lack-of-fit, and prediction error indices. Specifically, the index of fit squared (I^2) which quantifies the proportion of variability in the dependent variable explained by the retransformed model and is analogous to the coefficient of multiple determination, was employed as an overall goodness-of-fit measure (Eq. (6)). The degree of lack-of-fit was determined through an evaluation of the magnitude and temporal pattern of mean absolute biases ($\bar{B}_{a(k)}$; Eq. (7)) and mean relative biases ($\bar{B}_{r(k)}$; Eq. (8)) with respect to their 95% confidence intervals (Eq. (9); e.g., means with intervals not overlapping zero were considered indicative of the presence of bias). Predictive accuracy was evaluated employing prediction and tolerant intervals for both absolute and relative errors (Eqs. (10) and (11), respectively; Reynolds, 1984; Gribko and Wiant, 1992).

$$I^2_{(k)} = 1 - \frac{\sum_{l=1}^{L}\sum_{i=1}^{n(k)} (V_{(li)(k)} - \hat{V}_{(li)(k)})^2}{\sum_{l=1}^{L}\sum_{i=1}^{n(k)} (V_{(li)(k)} - \bar{V}_{(..)(k)})^2} \quad (6)$$

$$\bar{B}_{a(k)} = \frac{\sum_{l=1}^{L}\sum_{i=1}^{n(k)} (V_{(li)(k)} - \hat{V}_{(li)(k)})^2}{\sum_{l=1}^{L}\sum_{i=1}^{n(k)} li} \quad (7)$$

$$\bar{B}_{r(k)} = \frac{\sum_{l=1}^{L}\sum_{i=1}^{n(k)} \left(100\frac{(V_{(li)(k)} - \hat{V}_{(li)(k)})}{V_{(li)(k)}}\right)^2}{\sum_{l=1}^{L}\sum_{i=1}^{n(k)} li} \quad (8)$$

$$\bar{B}_{a,r(k)} \pm \frac{S_{a,r(k)} \cdot t_{(n(k)-1,0.975)}}{\sqrt{n_{(k)}}} \quad (9)$$

$$\bar{B}_{a,r(k)} \pm \sqrt{1/n_{(k)} + 1/n_p} \cdot S_{a,r(k)} \cdot t_{(n(k)-1,0.975)} \quad (10)$$

$$\bar{B}_{a,r(k)} \pm g(\lambda, n_{(k)}, P) \cdot S_{a,r(k)} \quad (11)$$

where $\hat{V}_{(li)_{(k)}}$ is the predicted cumulative moving average value for the kth attribute at the ith cambial age for the lth sample tree, and $n_{(k)}$ is the number of predicted-observed pairs specific to the kth attribute, $S_{a,r(k)}$ is the standard deviation of the absolute ($S_{a(k)}$) or relative ($S_{r(k)}$) biases specific to the kth attribute, $t_{(n(k)-1,0.975)}$ is the 0.975 quantile of the t-distribution with $n_{(k)} - 1$ degrees of freedom specific to the kth attribute, n_p is the number of future predictions considered (i.e., $n_p = 1$), and g is a normal distribution tolerance factor specifying the probability (λ) that at least a proportion of the distribution of errors (P; 95%) will be included within the stated tolerance interval. The temporal-based lack-of-fit and prediction error metrics were calculated for all cambial ages which had a minimum of 11 observational pairs (sensu Gribko and Wiant, 1992). A secondary data-centric measure of systematic bias as inferred from the linear relationship between the observed and predicted values, was also utilized (sensu Ek and Monserud, 1979). Lastly, for demonstration purposes and subsequent use in the SSDMMs, the final model

specifications were also parameterized deploying the full data set.

2.2. Model integration, attribute-based performance metrics, and simulations

The parameterized suite of hierarchical mixed-effects fibre attribute prediction equations were incorporated into the jack pine SSDMM structure via the introduction of a new Silviscan-based Fibre Attributes sub-module, as shown in Fig. 2. Given that the attribute equations deploy a cumulative size-dependent variate (final breast-height diameter), predictions were only generated for the rotational diameter distribution representing the final crop tree population. Additionally, in order to assess the magnitude of attribute variation for the harvestable trees within a given diameter class, attribute estimates were generated for cambial age 1 through N where N is the cambial age at rotation. These diameter-class-specific temporal sequences were then used to calculate measures of central tendency (mean) and variation (standard deviation and coefficient of variation). Stand-level attribute performance metrics were also calculated: i.e., diameter-class-based basal-area-weighted stand-level mean attribute values with associated relative measures of variation. Additionally, in order to introduce a comparative analysis among species, the suite of fibre attribute prediction models previously developed for black spruce (Newton, 2016), were also integrated into the upland black spruce SSDMM structure employing the identical procedure as that described for jack pine.

The utility of the resultant enhanced SSDMMs was demonstrated by generating and comparing rotational fibre attribute outcomes for a set of operationally-relevant crop plans. Specifically, the following 4 scenarios were considered: (1&2) unthinned natural-origin jack pine and black spruce stands which established following a stand-replacing disturbance at high densities (5000 stems/ha) on medium-to-good quality sites (site index = 18 m @ 50 years (breast-height age) (Carmean et al., 2001, 2006)); and (3&4) unthinned jack pine and black spruce plantations which were established using improved stock (genetic worth effects of 7% at a selection index age of 20 years for jack pine, and 10% at a selection index age of 15 years for black spruce (sensu Newton, 2003)) at conventionally-deployed densities of 2500 stems/ha on scarified harvested sites of medium-to-good quality (site index = 18 m @ 50 years (breast-height age) (Carmean et al., 2001, 2006)). Identical rotational lengths and operational adjustment factors for density-independent mortality were used for all 4 simulations: i.e., 50 years and 0.01%/yr, respectively.

3. Results

3.1. Hierarchical mixed-effects fibre attribute prediction equations

3.1.1. Model specifications, parameter estimates and compliance with underlying statistical assumptions

Attribute-specific parameter estimates and associated regression statistics including the results from the assessment of serial correlation are presented in Table 2. The resultant models included only significant ($p \leq 0.05$) random and fixed effects as determined from univariate and multivariate tests of significance, and exploratory analysis of second-stage predictors (sensu Raudenbush and Bryk, 2002). Random effects that were determined to be significant ($p \leq 0.05$) were indicative of the presence of random variation among individual trees that could be partially explained by the second-stage fixed-effect predictor variable (cumulative breast-height diameter at time of sampling). The results from the serial correlation assessment deploying autocorrelation coefficients in conjunction with the Box-Ljung statistic, indicated there was evidence of the presence of first-order serial correlation among consecutive first-level Bayes residual values for a proportion of the attribute-specific sequences (Table 2): 18, 23, 26, 28, 28, 30, 31 and 57% of the D_r, S_a, C_o, M_e, D_t, W_t, W_d and M_a residual sequences exhibited significant ($p \leq 0.01$) correlation, respectively. Although further remedial efforts in terms of iteratively removing additional observations from the sequences in order to create smaller calibration data subsets may reduce the occurrence of serial correlation, this approach could also compromise model specification (e.g., yielding insufficient observations to explicitly reflect the size-dependent non-linear temporal trends present within the trajectories (Fig. 1)). Consequently, no further remedial efforts were exercised given that approximately 65% of the original observations within the individual tree sequences had already been removed.

Graphical examination of residual scatterplots which revealed no evidence of systematic bias supported the non-rejection of the homogeneity of variance assumption. The potential effect of thinning on the 2nd level parameter estimates was assessed using the exploratory analysis option within the HLM7 software program (sensu Raudenbush and Bryk, 2002): generating approximate Student t-to-enter statistics for plausible but excluded 2nd level variables on each of the attribute-specific random parameters ($\beta_{0,1,2}$). Results indicated that thinning effects would be inconsequential if included in terms of influencing the overall fibre attribute trajectories (i.e., Student t-values were much less than the critical threshold value). In terms of explanatory power, the proportion of variation explained by the models was 74, 72, 72, 65, 60, 57, 55, and 28% for C_o, M_e, W_t, S_a, W_d, M_a, D_r and D_t, respectively (as measured by the index of fit (Table 2)). Furthermore, graphical examination of the observed versus predicted values for each attribute-specific regression relationship (not shown) revealed that most values fell within close proximity to the diagonal line of equivalence.

3.1.2. Model performance indicators: goodness-of-fit, lack-of-fit and predictive ability

The goodness-of-fit, lack-of-fit, and prediction error indices generated employing the validation data subset, are provided in Table 3. The values of the goodness-of-fit metric, I^2, were indicative of acceptable levels of explanatory power in terms of the percent of variation explained by the models: 75, 71, 71, 66, 60, 55, 49, and 38% for C_o, M_e, W_t, S_a, W_d, M_a, D_r and D_t, respectively. These values are similar to those for the models parameterized using the calibration data subset (Table 2) and revealed an identical order when sorted on the basis of magnitude. Furthermore, graphical examination of these relationships in terms of their residual patterns did not reveal the presence of consequential outliers or influential observations. The secondary measure of systematic bias employing the observed-predicted regression relationships, indicated that the intercept and slope values were not significantly ($p \leq 0.05$) different from zero and unity, respectively, for 6 of the 8 attributes (Table 3). Only the models for W_t and D_t failed to meet this criterion.

Lack-of-fit was assessed via the graphical examination of the temporal pattern of absolute and relative biases with increasing cambial age. Specifically, Fig. 3a illustrates the attribute-specific temporal trends in mean absolute bias with associated 95% confidence intervals whereas Fig. 3b presents attribute-specific temporal patterns in mean relative bias and associated 95% confidence intervals. Examination of the absolute and relative biases on an individual attribute basis indicated the absence of systematic lack-of-fits. Furthermore, with very few exceptions, the biases were not significantly ($p \leq 0.05$) different from zero, as inferred by the lack of non-overlapping confidence intervals (e.g., inconsequential annual exceptions being the absolute and (or) relative biases for W_d, C_o, W_t, D_r, D_t and S_a at cambial age 3, and those for W_d, W_t, D_r, and S_a at cambial age 67). Although exceptions infrequently occurred at the end of the age range considered (e.g., biases for M_a and M_e at cambial age 69), the relative biases did not exceed ± 10% for the majority of the cambial ages assessed. Comparisons among the attributes in terms of relative biases indicated that the model developed for M_a exhibited the greatest range whereas the model developed for D_r exhibited the least. The increased width of the confidence intervals for both absolute and relative biases at cambial ages greater than 50 years for all 8 attributes was partially due to the

Table 2
Parameter estimates and associated statistics for the attribute-specific hierarchical mixed-effects models (Eq. (5)) parameterized employing the calibration data subset.

Attribute[a]	Parameter estimate[b]									Statistics[c]		
	β'_{00}	β_{00}	β_{01}	β_{10}	β_{11}	β_{20}	β_{21}	β_{30}	β_{31}	*SEE*	$n_{\alpha(1)}$ (%)	I^2
W_d	347.6651	5.851100	–	−0.014900	–	0.005606	0.000155	-0.000068	–	0.014	19 (31)	0.602
M_a	31.2562	3.441706	0.011445	−0.269022	–	−0.002842	–	0.000059	–	0.032	35 (57)	0.569
M_e	2.5038	0.916984	–	0.465419	–	−0.00999	0.000273	−0.000011	–	0.041	17 (28)	0.719
C_o	226.4852	5.422567	–	0.214446	−0.003076	−0.005823	0.000365	−0.000038	–	0.015	16 (26)	0.738
W_t	1.7119	0.537494	–	0.125281	−0.002682	−0.000389	0.000350	−0.000066	–	0.016	18 (30)	0.717
D_r	33.5959	3.514372	−0.021775	0.017324	0.008901	−0.007113	−0.000243	0.000074	–	0.008	11 (18)	0.546
D_t	21.2310	3.055431	0.008212	0.115254	−0.005140	−0.001950	0.000217	−0.000028	–	0.008	17 (28)	0.279
S_a	413.5901	6.024791	–	−0.023824	–	−0.003009	−0.000177	0.000059	–	0.013	14 (23)	0.647

[a] W_d, M_a, M_e, C_o, W_t, D_r, D_t and S_a denote wood density, microfibril angle, modulus of elasticity, fibre coarseness, tracheid wall thickness, tracheid radial diameter, tracheid tangential diameter and specific surface area, respectively.

[b] Attribute-specific parameter estimates obtained from hierarchical mixed-effects regression analyses. Note, the intercept parameter estimates includes a correction factor for the bias introduced via the logarithmic transformation (Sprugel, 1983): $\beta'_{00} = e^{\beta_{00}+SEE^2/2}$.

[c] *SEE* denotes the standard error of estimate in natural logarithmic units specific to the *k*th attribute (Table 1); $n_{\alpha(1)}$ is the number of highly significant ($p \leq 0.01$) first-order autocorrelation coefficients ($\alpha(1)$) between consecutive residual values at the individual tree level for the 61 sample trees; I^2 is the index of fit squared (Eq. (6)).

systematic reduction in the number of sample observations available. This sampling artifact arose principally from the differential in total stand age between the 2 sampling sites: the sample trees from the Sewell site had a maximum age of 51 compared to the sample trees from the Tyrol site which had a maximum age of 71. Consequently, the total number of values declined from 61 to 30 at an approximate cambial age of 52.

Predictive accuracy was assessed using absolute and relative prediction and tolerance error intervals (Reynolds, 1984; Gribko and Wiant, 1992). Table 3 provides attribute-specific 95% prediction and tolerance limits for both error types across all cambial ages and tree sizes. The prediction interval quantifies the precision of the equations in terms of predicting fibre attributes for a newly sampled tree: specifically, there is a 95% probability that the error generated from a single new prediction would fall between the specified limits. Examining the resultant intervals indicated that there was a differentiation among the attributes in terms of the absolute width of their relative intervals: $D_t < D_r < S_a < W_d < C_o < W_t < < M_e < < < M_a$. Overall, however, for both interval types, absolute and relative mean errors were not significantly ($p \leq 0.05$) different from zero, indicating that the models would generate unbiased predictions.

The temporal trend of the mean absolute and relative prediction errors along with their 95% confidence intervals, are presented in Figs. 4a and 4b, respectively. The attribute-specific temporal patterns and the magnitude of the errors among the attributes were interpreted as follows: (1) with very few exceptions, prediction errors were not significantly ($p \leq 0.05$) different from zero as inferred by overlapping prediction intervals (i.e., intervals intersecting the horizontal null-line); (2) the majority of relative errors did not exceed ± 10% for D_t, ± 15% for W_d, C_o, D_r, and S_a, ± 20% for M_a and W_t, and ± 60% for M_e; and (3)

Table 3
Goodness-of-fit and lack-of-fit statistics and overall predictive ability of the transformed attribute-specific hierarchical mixed-effects models.

Attribute[a]	Goodness-of-fit statistics			Lack-of-fit measures[d]				Predictive ability: 95% error intervals[f]			
	I^2[b]	Hypotheses[c]		Absolute[e]		Relative (%)		Prediction interval		Tolerance interval	
		$\alpha_0 = 0$	$\alpha_1 = 1$	Mean bias	95% CL	Mean bias	95% CL	Absolute[e] 95% CL	Relative (%) 95% CL	Absolute[e] 95% CL	Relative (%) 95% CL
W_d	0.597	H_0	H_0	−2.186*	± 0.992	−0.180	± 0.244	± 47.304	± 11.620	± 48.600	± 11.937
M_a	0.545	H_0	H_0	−0.223*	± 0.138	2.704*	± 0.853	± 6.576	± 40.647	± 6.756	± 41.757
M_e	0.706	H_0	H_0	−0.179	± 0.064	0.863*	± 0.711	± 3.046	± 33.890	± 3.129	± 34.817
C_o	0.752	H_0	H_0	−1.317*	± 0.914	−0.001	± 0.245	± 43.547	± 11.669	± 44.737	± 11.988
W_t	0.714	H_1	H_1	−0.017*	± 0.007	−0.247	± 0.262	± 0.316	± 12.475	± 0.324	± 12.816
D_r	0.490	H_0	H_0	0.024	± 0.052	0.258*	± 0.174	± 2.498	± 8.275	± 2.566	± 8.501
D_t	0.377	H_1	H_0	−0.022	± 0.030	−0.010	± 0.111	± 1.430	± 5.275	± 1.469	± 5.420
S_a	0.656	H_0	H_0	0.799*	± 0.762	0.545*	± 0.227	± 36.330	± 10.835	± 37.322	± 11.131

[a] As defined in Table 2.

[b] As defined in Table 2.

[c] Based on the simple linear regression relationship between transformed observed (y) and predicted (x) values ($y = \alpha_0 + \alpha_1 x + \varepsilon$ where ε is an error term), testing the (1) null hypotheses that $\alpha_0 = 0$ versus the alternative hypothesis $\alpha_0 \neq 0$ where H_0 and H_1 denote the non-rejection and rejection of the null hypothesis at the 0.05 probability level, respectively, and (2) null hypotheses that $\alpha_1 = 1$ versus the alternative hypothesis $\alpha_1 \neq 1$ where H_0 and H_1 denote the non-rejection and rejection of the null hypothesis at the 0.05 probability level, respectively.

[d] Mean absolute (Eq. (7)) and relative (Eq. (8)) bias and the limits (CL) of the associated 95% confidence interval (Eq. (9)) where mean values significantly ($p \leq 0.05$) different from zero (denoted by superscript *) were suggestive of a potentially biased relationship.

[e] Absolute error units are specific to each attribute: kg/m^3, °, GPa, µg/m, µm, µm, µm, and m^2/kg for W_d, M_a, M_e, C_o, W_t, D_r, D_t and S_a, respectively.

[f] Confidence limit(s) (CL) for the 95% prediction and tolerance error intervals for absolute and relative errors (Eqs. (10) and (11), respectively): mean bias ± 95% CL. Note: (1) there is a 95% probability that the a future error will be within the stated prediction interval; (2) there is a 95% probability that 95% of all future errors will be within the stated tolerance interval; and (3) underlined values indicate approximations given non-normality within the underlying error distribution (sensu Reynolds, 1984; Gribko and Wiant, 1992).

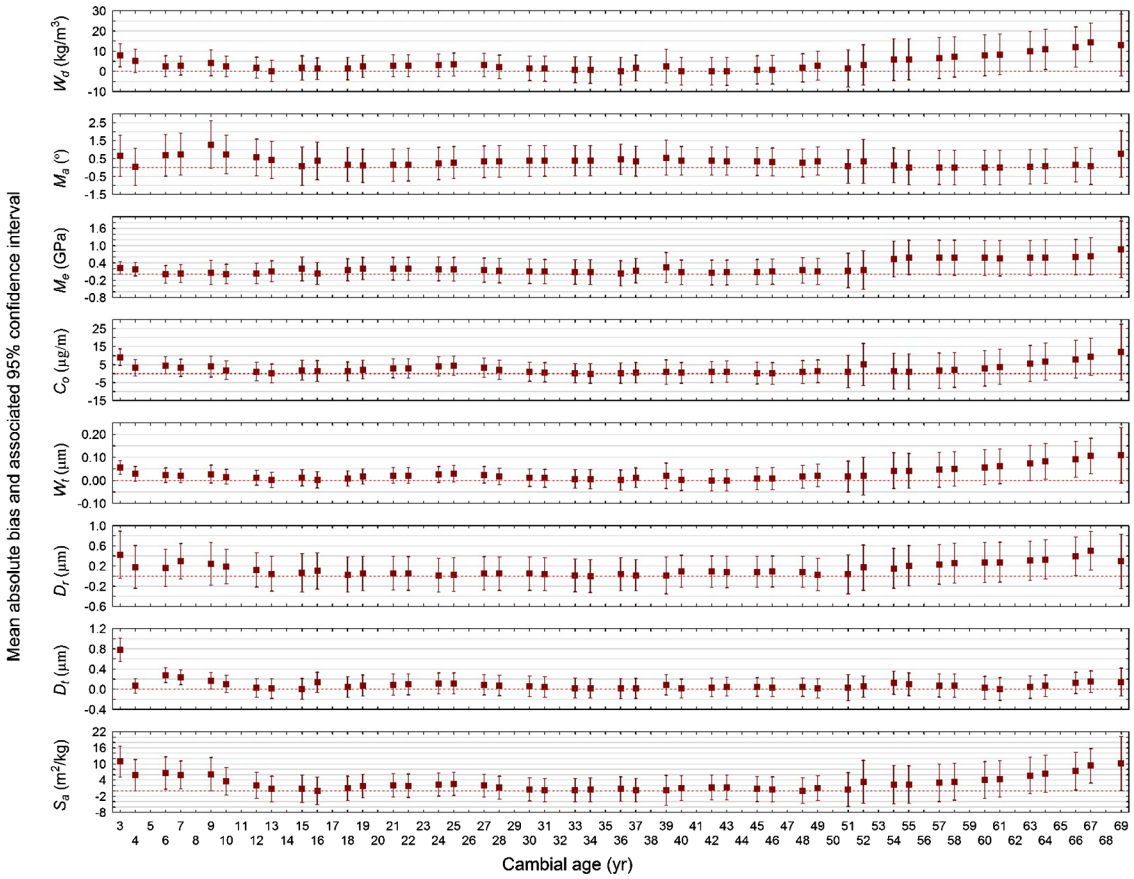

Fig. 3a. Model evaluation – lack-of-fit analysis: attribute-specific temporal profiles of mean absolute bias with associated 95% confidence intervals.

there was a lack of systematic temporal trends for both error types irrespective of attribute. Even though the parameterized specifications exhibited no systematic trends, the magnitude of relative errors did vary among attributes: $D_t < W_d$, C_o, D_r, $S_a < M_a$, $W_t < < M_e$. Although not shown, the temporal patterns in both the absolute and relative tolerance error intervals were consistent with the results observed for the prediction error intervals. The only overall difference was that, as expected, the values for the tolerance error intervals were slightly greater in magnitude than those observed for the corresponding prediction error intervals (n., comparison of the composite values for the prediction and tolerance error intervals for all ages combined, as shown in Table 3, is also in agreement with this graphical-derived inference).

3.1.3. Presentation and interpretation of size-dependent temporal developmental trajectories

Table 4 provides the parameter estimates and associated regression statistics for the final model forms parameterized employing the full data set. Overall, the parameter values were similar in terms of their sign and magnitude to those estimated using the calibration data subset (cf. Table 2 with Table 4). Likewise, contrasting the standard error of estimates and the index-of-fit metrics from Table 4 to those reported in Table 2, revealed that the magnitude of the regression statistics were also comparable. Fig. 5 exemplifies the size-dependent nature of developmental variation for each attribute, as predicted from the two-stage hierarchical mixed-effects models parameterized using the full data set. Although non-linear cumulative-based developmental trajectories were observed for all attributes irrespective of tree-size, the trajectories did exhibit size-related temporal differentiation in terms of curve shape and rate of change.

Specifically, the trajectories for W_d and M_e exhibited temporally increasing separation in which values varied directly with tree size: smaller-sized trees exhibited lower wood density and stiffness values than those predicted for larger-sized trees for any given age and the differences increased with cambial age. The trajectories for M_a exhibited a minimal size-dependent effect that was relatively temporally invariant (e.g., smaller-sized trees having a slightly lower microfibial angle than larger-sized trees for any given age). The trajectories for C_o and W_t where similar in that both followed the same initial pathway with minimal size-dependency until intersecting briefly at cambial ages of approximately 30 and 25, respectively. Thereafter, dramatically exhibiting increasingly size-dependent divergence with increasing cambial age: e.g., the smallest sized tree attained substantially lower fibre coarseness and tracheid wall thickness values than that attained by the largest sized tree and the difference increased with cambial age. The most complex set of size-dependent trajectories among all 8 attributes were those for D_t. Specifically, the D_t trajectories exhibited 2 intersection points and an associated size-dependence reversal where the inversely proportional relationship with tree size observed over the 10–50 year range become directly proportional thereafter. Although the trajectories for S_a exhibited rapid initial declines followed by an upward trend with increasing cambial age for all 3 tree sizes, the smallest size tree exhibited the highest cumulative values at any given age with the size-dependent differential increasing with age. Among all the attribute trajectories examined, only those for M_a and D_r exhibited decreasing size-dependence with increasing age.

3.2. Resultant enhanced SSDMMs and their exemplification in crop planning

The parameterized fibre attribute prediction equations when incorporated into the SSDMM structure via the new Silviscan-based Fibre Attributes sub-module (Fig. 2), enabled the generation of attribute estimates and associated composite metrics at the diameter class and

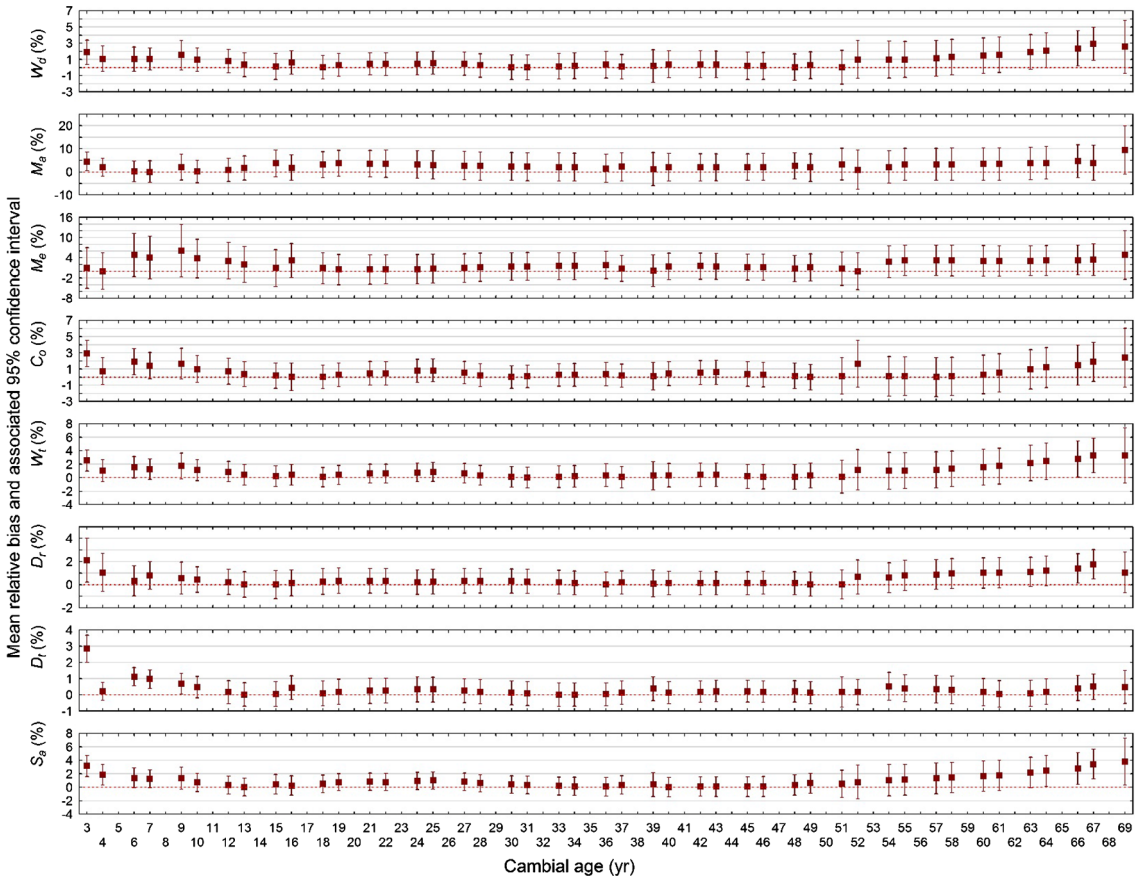

Fig. 3b. Model evaluation – lack-of-fit analysis: attribute-specific temporal profiles of mean relative bias with associated 95% confidence intervals.

stand levels. Essentially, for a given crop plan, the grouped-diameter distribution outputted from the Diameter and Height Recovery Module along with age information are used to generate rotational attribute estimates for each diameter class, deploying the parameterized models. For example, Table 5 provides the resultant diameter-class-specific and stand-level fibre outcome metrics for the 4 crop plans selected to exemplified the utility of the enhanced SSDMMs.

Examination of the size-dependent attribute-specific trends for the jack pine crop plans, indicated that the solid-wood end-product potential increased with increasing tree size (e.g., increasing W_d, M_e and W_t values with increasing diameter class). Conversely, for the black spruce crop plans, solid-wood end-product potential declined with increasing tree size (e.g., decreasing W_d, M_e, and W_t values with increasing diameter class). For both species, although pulp and paper end-product potential increased with increasing tree size according to some attributes (e.g., increasing C_o values with increasing diameter class), the trends were not as definitive as those presented for the solid-wood related attributes. Additionally, in order to broaden the discussion in terms of addressing both the quality and quantity of fibre produced, rotational volumetric-related yield metrics (stand density, and chip and lumber volumes) are provided in Table 6. It is evident from the results for both species, initial spacing had a large effect on stand structure (grouped-diameter frequency distribution) and associated product volumes relative to the untreated natural-origin stands. Essentially, initial spacing shifted the diameter distribution towards the larger diameter classes resulting in greater product volumes at both the diameter class and stand levels. For example, at the stand-level, the jack pine and black spruce plantations respectively produced 55% and 33% greater chip volumes, and 80% and 120% greater lumber volumes, than did their natural-origin stand counterparts. Although these comparisons are specific to the crop plan configurations selected for exemplification, the results are in general accordance with expectation: i.e., reduced intraspecific competition over the rotation due to regulating spatial patterns and overall site occupancy via initial spacing, results in higher individual tree growth rates and lower rates of competition-induced mortality that ultimately leads to greater volumetric product yields at rotation.

Inferring wood quality and associated end-product potential directly from internal fibre attributes of standing boreal coniferous species is challenging due to the lack of relationships that explicitly link tree-based attribute values to those within the derived end-products, and attribute-based design specifications for a given end-product. Consequently, 2 alternative implicit-based approaches were deployed in this study: (1) utilizing species-specific sample-based mean attribute values derived from surveys and experiments in order to formulate population-like reference estimates; and (2) using lumber grading guidelines to extract a plausible range of attribute values that can be presumptively deployed to delineate standing crop trees into specific grade classes. With respect to the first approach, Silviscan-based attribute values determined from breast-height radial xylem samples obtained from 61 trees sampled within natural-origin semi-mature and mature jack pine stands (this study; Table 1) along with a similar attribute set derived from 111 trees sampled within natural-origin semi-mature and mature black spruce stands distributed throughout the study region (central portion of the Canadian Boreal Forest Region (Rowe, 1972) as referenced in Newton, 2016) where used to established species-specific population-like mean estimates. Specifically, the mean attribute values generated from these samples were as follows: (1) 438 kg/m^3, 13.9°, 12.5 GPa, 412 μg/m, 2.8 μm, 30.8 μm, 27.7 μm, and 309 m^2/kg for W_d, M_a, M_e, C_o, W_t, D_r, D_t, and S_a, respectively, for jack pine; and (2) 537 kg/m^3, 12.8°, 14.9 GPa, 375 μg/m, 2.6 μm, 27.6 μm, 26.4 μm, and 301 m^2/kg for W_d, M_a, M_e, C_o, W_t, D_r, D_t, and S_a, respectively, for black spruce. Contrasting these sample based means with model-based outputs provides a reference point for evaluating the

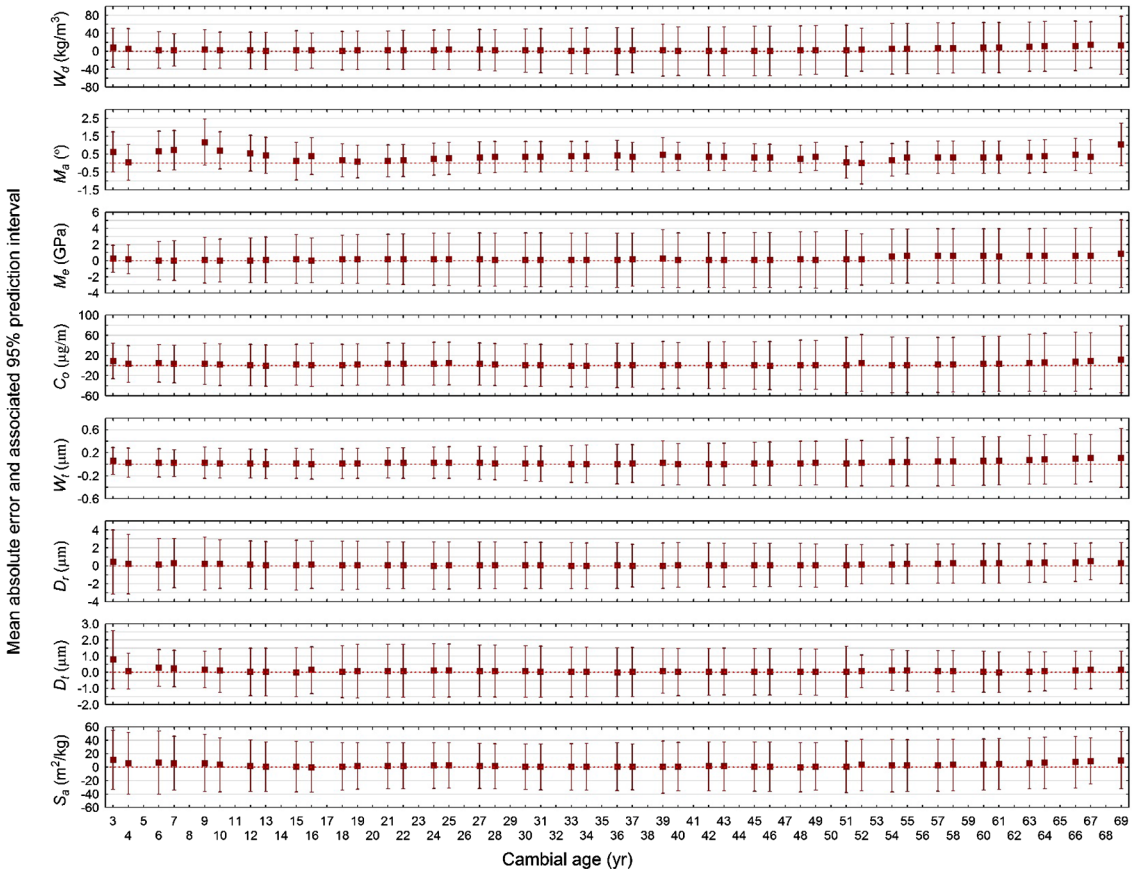

Fig. 4a. Model evaluation – predictive ability: attribute-specific temporal profiles of mean absolute prediction error with associated 95% intervals.

quality of attributes produced for a given crop plan. For example, comparing these values against the stand-level mean estimates as shown in Table 5, revealed that the selected jack pine crop plans produced wood of slightly lower quality in terms of both solid-wood, and pulp and paper, end-product potentials: e.g., ≈6% decline in wood density, ≈5% increase in microfibrial angle, ≈11% decrease in stiffness (modulus of elasticity), ≈5% reduction in fibre coarseness, and ≈8% decline in cell wall thickness. Similar contrasts in regards to the black spruce crop plans indicated much more dramatic declines in end-product potentials, particularly with respect to the plantation: e.g., ≈21% reduction in wood density, ≈30% increase in microfibrial angle, ≈32% decline in stiffness (modulus of elasticity), ≈13% reduction in fibre coarseness, and ≈23% decline in cell wall thickness.

The second approach can be exemplified by contrasting the diameter-class attribute predictions to corresponding threshold values derived from grading rules which are used operationally to define end-product type and grade. For example, for solid-wood end-products (dimensional lumber) derived from sawlog-sized trees (diameter-classes ≥ 14 cm), an estimate of grade category based on the modulus of elasticity and wood density can be extracted from the SPS-2 design standard issued by the National Lumber Grade Authority (NLGA) for the spruce-pine-fir species group. Presuming approximate equivalence between Silviscan-based modulus of elasticity estimates within standing trees and the static modulus of elasticity within extracted dimensional lumber, 3 grade groupings were derived from the design specifications given in Table 2 of the NLGA standard for machine stress-rated (MSR) lumber (NLGA, 2013): (1) low MSR grade class grouping (1.2E to 1.7E) as defined as sawlog-sized trees having a M_e value in the range of > 8.3 to 12.1 GPa, and a W_d value in the range of > 400 to 440 kg/m^3; (2) medium MSR grade class grouping (1.8E to 1.9E) as defined as sawlog-sized trees having a M_e value in the range of > 12.1 to 13.5 GPa, and a W_d value in the range of > 440 to 480 kg/m^3; and (3) high MSR grade class grouping (2.0E to 2.4E) as defined as sawlog-sized trees having a M_e value in the range of > 13.5 to 16.5 GPa, and a W_d value in the range of > 480 to 520 kg/m^3. Although design specifications for the other attributes are not officially specified, trees within diameter-classes for which the M_a mean value is greater than 15° were tagged as potentially problematic in terms their pulp and paper, and solid-wood end-product potentials. These grade classes when applied to the rotational diameter distributions generated for the 4 crop plans (Table 5) suggested that lumber end-product potential would varied considerably with tree size and species. For example, the grade of lumber produced from the sawlog-sized (≥14 cm diameter class) jack pine trees would fall within the low quality class but systematically increase with increasing tree size. Conversely, the grade of lumber extracted from sawlog-sized black spruce trees would systematically decline from high to low with increasing tree size. In collective consideration of these wood quality attribute predictions along with rotational estimates of stand densities, and lumber and chip volumes produced, suggested that the jack pine plantation would yield a greater number of higher quality crop trees and associated product volumes (75%) than its natural-origin stand counterpart (Table 6). This could potentially translate into overall increases in the quality and quantity of derived end-products. Although the black spruce plantation would similarly produced a greater number of larger-sized crop trees and product volumes (75%) than its natural-origin stand counterpart (Table 6), the overall quality of the wood produced would be inferior. Furthermore, the high microfibril angles (> 15°) for the largest diameter classes (≥22 cm) with the plantation

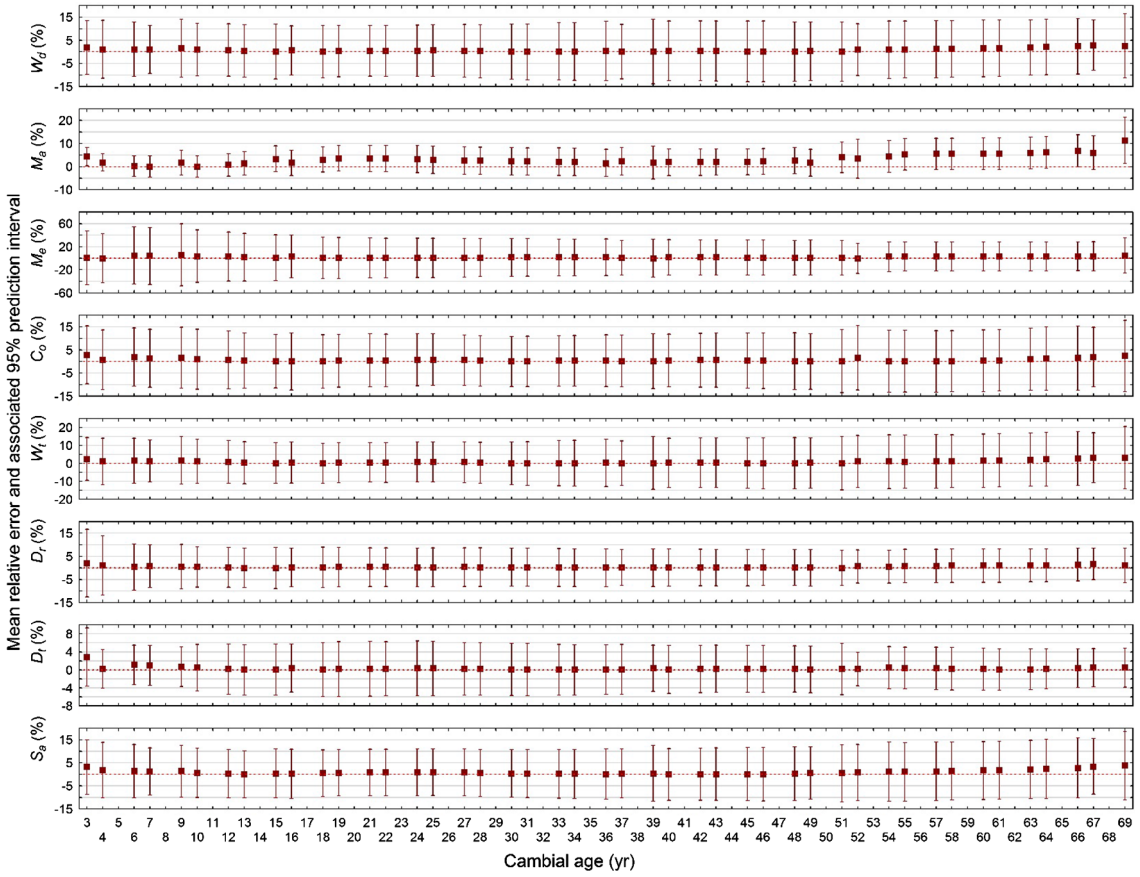

Fig. 4b. Model evaluation – predictive ability: attribute-specific temporal profiles of mean relative prediction error with associated 95% intervals.

would also negatively affect end-product potential.

4. Discussion

4.1. Size-dependent temporal developmental trajectories of commercially-relevant fibre attributes

The final parameterized model specifications reflect the attribute-specific and size-dependent developmental trajectories of 8 primary fibre-based determinates of end-product potential (Table 2; Fig. 5): specifically, wood density, microfibril angle, modulus of elasticity, fibre coarseness, tracheid wall thickness, tracheid radial diameter, tracheid tangential diameter and specific surface area (sensu Defo, 2008). Statistically, the jack pine models (1) explained a moderate proportion of the variation in the dependent variables (i.e., ranging from a minimum of 38% for D_t to a maximum of 75% for C_o as quantified by the index of fit metric; Table 3), (2) exhibited no consequential patterns of systematic lack-of-fit (Fig. 3a and 3b), and (3) generated relatively precise predictions ($\leq \pm$ 13%) for all attributes except M_a and M_e (Table 3; Figs. 4a and 4b). These goodness-of-fit, lack-of-fit and predictive performance measures reconfirm the utility of a two-stage hierarchical mixed-effects model specification for describing size-dependent fibre attribute developmental trends of boreal conifers. Previously, Newton (2016) deployed a similar modelling approach for quantifying the temporal attribute developmental trajectories for plantation black spruce trees. Specifically, utilizing a two-level hierarchical model specification with random and fixed effects where Hoerl's (1954) compound exponential regression model was deployed at the 1st level, and tree size (cumulative diameter) was employed as the 2nd level predictor variable. Although the models for the black spruce attributes were

Table 4
Parameter estimates and associated statistics for the attribute-specific hierarchical mixed-effects models (Eq. (5)): parameterized employing the full data set.

Attribute[a]	Parameter estimate[b]									Statistics[c]	
	β'_{00}	β_{00}	β_{01}	β_{10}	β_{11}	β_{20}	β_{21}	β_{30}	β_{31}	*SEE*	I^2
W_d	353.9963	5.869174	–	−0.028030	–	0.006781	0.000157	−0.000079	–	0.015	0.597
M_a	29.9767	3.399737	0.009902	−0.220091	–	−0.006925	–	0.000092	–	0.037	0.545
M_e	2.5613	0.939504	–	0.445814	–	−0.008902	0.000322	−0.000031	–	0.045	0.706
C_o	252.6516	5.531747	–	0.157867	−0.003968	−0.001039	0.000454	−0.000097	–	0.023	0.752
W_t	1.8163	0.596596	–	0.093448	−0.003134	0.002349	0.000396	−0.000098	–	0.019	0.714
D_r	29.6195	3.388374	−0.015729	0.072807	0.006254	−0.008989	−0.000154	0.000074	–	0.011	0.490
D_t	19.5205	2.971323	0.017443	0.141691	−0.009895	0.000110	0.000428	−0.000082	–	0.017	0.377
S_a	391.3092	5.969370	–	0.014559	–	−0.006120	−0.000192	0.000089	–	0.016	0.656

[a] As defined in Table 2.
[b] As defined in Table 2.
[c] As defined in Table 2.

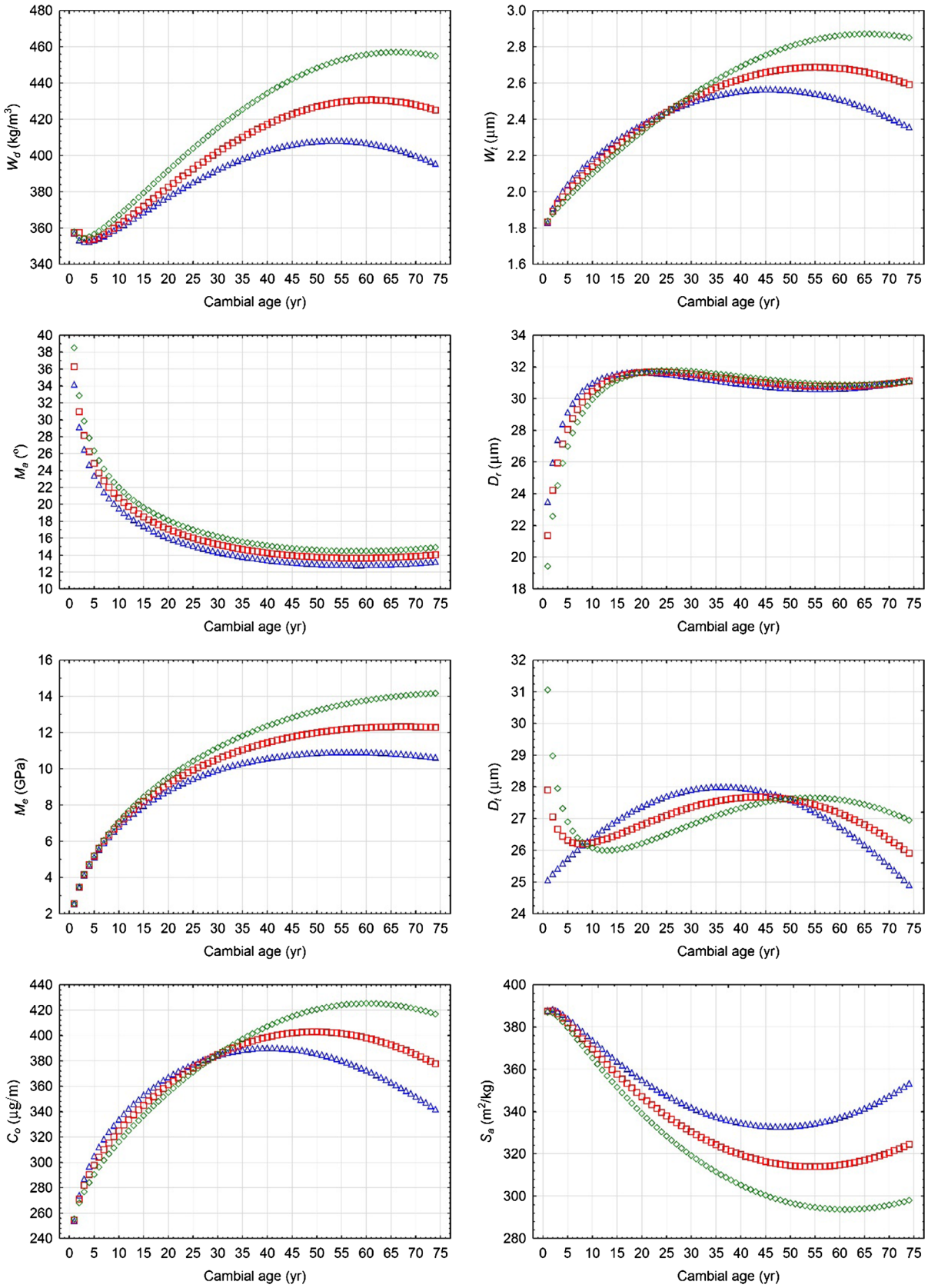

Fig. 5. Size-dependent temporal developmental trends of cumulative area-weighted mean values by attribute as described by the models parameterized employing the full data set (Table 4): triangles, squares and diamonds denote the trends for small (d_b = 14), medium (d_b = 20) and large (d_b = 26) diameter trees, respectively.

Table 5
Rotational diameter-class and associated stand-level fibre attribute outcomes for natural-origin and plantation jack pine and black spruce stand-types situated on medium-to-good quality sites as predicted by the enhanced SSDMMs.

Attribute[a]	Stand-	Stand-level		Rotational diameter class (cm)[d]													
(unit)	type[b]	$\bar{x}$[c]	CV	2	4	6	8	10	12	14	16	18	20	22	24	26	28
W_d	$PNb_{(N)}$	$402^{[-8]}$	4.7	373	378	384	389	395	401	**407**	**413**						
(kg/m^3)	$PNb_{(P)}$	$423^{[-3]}$	6.0				389	395	401	**407**	**413**	**419**	**425**	**432**	**438**		
	$PIm_{(N)}$	$486^{[-9]}$	7.5	584	566	549	533	517	501	*486*	***472***	***457***					
	$PIm_{(P)}$	$426^{[-21]}$	9.2				533	517	501	*486*	***472***	***457***	**444**	**430**	**418**	**405**	393
M_a	$PNb_{(N)}$	$12.8^{[+8]}$	28.1	11.6	11.8	12.1	12.3	12.6	12.8	13.1	13.3						
(°)	$PNb_{(P)}$	$13.7^{[+1]}$	27.1				12.3	12.6	12.8	13.1	13.3	13.6	13.9	14.1	14.4		
	$PIm_{(N)}$	$11.6^{[+9]}$	27.8	6.9	7.5	8.1	8.9	9.7	10.5	11.4	12.4	13.5					
	$PIm_{(P)}$	$16.7^{[-30]}$	18.9				8.9	9.7	10.5	11.4	12.4	13.5	14.7	**16**	**17.4**	**19**	20.6
M_e	$PNb_{(N)}$	$10.5^{[-16]}$	25.8	9	9.3	9.6	9.9	10.2	10.5	**10.8**	**11.2**						
(GPa)	$PNb_{(P)}$	$11.7^{[-6]}$	27.0				9.9	10.2	10.5	**10.8**	**11.2**	**11.5**	**11.9**	**12.2**	**12.6**		
	$PIm_{(N)}$	$15.1^{[+1]}$	22.1	25.9	23.7	21.6	19.7	18	16.5	*15*	***13.7***	***12.5***					
	$PIm_{(P)}$	$10.2^{[-32]}$	14.7				19.7	18	16.5	*15*	***13.7***	***12.5***	**11.4**	**10.5**	**9.5**	**8.7**	8.0
C_o	$PNb_{(N)}$	$384^{[-7]}$	9.8	361	365	370	374	379	384	388	393						
(μg/m)	$PNb_{(P)}$	$401^{[-3]}$	10.9				374	379	384	388	393	398	403	408	412		
	$PIm_{(N)}$	$284^{[-24]}$	10.3	231	239	247	256	265	274	283	293	303					
	$PIm_{(P)}$	$328^{[-13]}$	12.9				256	265	274	283	293	303	313	324	335	347	359
W_t	$PNb_{(N)}$	$2.5^{[-11]}$	8.5	2.4	2.4	2.4	2.5	2.5	2.5	2.6	2.6						
(μm)	$PNb_{(P)}$	$2.7^{[-4]}$	9.9				2.5	2.5	2.5	2.6	2.6	2.6	2.7	2.7	2.7		
	$PIm_{(N)}$	$2.2^{[-15]}$	7.3	2.5	2.4	2.4	2.4	2.3	2.3	2.2	2.2	2.1					
	$PIm_{(P)}$	$2.0^{[-23]}$	7.2				2.4	2.3	2.3	2.2	2.2	2.1	2.1	2.0	2.0	2.0	1.9
D_r	$PNb_{(N)}$	$30.7^{[-0]}$	4.7	30.3	30.4	30.5	30.5	30.6	30.7	30.7	30.8						
(μm)	$PNb_{(P)}$	$30.9^{[+0]}$	6.5				30.5	30.6	30.7	30.7	30.8	30.9	30.9	31	31.1		
	$PIm_{(N)}$	$23.7^{[-14]}$	8.9	19.6	20.2	20.9	21.5	22.2	22.9	23.7	24.4	25.2					
	$PIm_{(P)}$	$27.2^{[-1]}$	11.0				21.5	22.2	22.9	23.7	24.4	25.2	26	26.9	27.7	28.6	29.5
D_t	$PNb_{(N)}$	$28.1^{[+1]}$	4.2	28.2	28.2	28.2	28.1	28.1	28.1	28	28						
(μm)	$PNb_{(P)}$	$28.0^{\{+1\}}$	2.6				28.1	28.1	28.1	28	28	28	27.9	27.9	27.9		
	$PIm_{(N)}$	$24.4^{[-8]}$	6.4	22.6	22.9	23.2	23.5	23.8	24.1	24.4	24.7	25					
	$PIm_{(P)}$	$25.8^{[-2]}$	7.1				23.5	23.8	24.1	24.4	24.7	25	25.4	25.7	26	26.4	26.7
S_a	$PNb_{(N)}$	$338.6^{[+10]}$	5.0	371	364	358	352	345	339	333	327						
(m^2/kg)	$PNb_{(P)}$	$318.0^{[+3]}$	6.6				352	345	339	333	327	321	315	310	304		
	$PIm_{(N)}$	$357.9^{[+19]}$	6.0	363	362	361	360	360	359	358	357	356					
	$PIm_{(P)}$	$354.4^{[+18]}$	6.4				360	360	359	358	357	356	356	355	354	353	352

[a] As defined in Table 2.

[b] $PNb_{(N)}$ and $PNb_{(P)}$ denote natural-origin and plantation jack pine stand-types whereas $PIm_{(N)}$ and $PIm_{(P)}$ denote natural-origin and plantation upland black spruce stand-types, respectively.

[c] Bracketed superscript values denote the magnitude of the stand-level mean relative differences (%) and their potential end-product related consequences (positive (+) or negative (−)) between the predicted attribute values produced for the specified crop plans and those derived from sample-based surveys (i.e., attribute-specific sample-based values for jack pine (this study) and black spruce (Newton, 2016) were respectively, 438 and 537 for W_d (kg/m^3), 13.9 and 12.8 for M_a (°), 12.5 and 14.9 for M_e (GPa), 412 and 375 for C_o (μg/m), 2.8 and 2.6 for W_t (μm), 30.8 and 27.6 for D_r (μm), 27.7 and 26.4 for D_t (μm), and 309 and 301 for S_a (m^2/kg)).

[d] Projected lumber grade grouping for trees within diameter classes of sawlog size (≥14 cm): (1) low MSR grade class grouping (1.2E to 1.7E) as defined as sawlog-sized trees having a M_e value in the range of > 8.3 to 12.1 GPa and a W_d value in the range of > 400 to 440 kg/m^3 are denoted via a bold font; (2) medium MSR grade class grouping (1.8E to 1.9E) as defined as sawlog-sized trees having a M_e value in the range of > 12.1 to 13.5 GPa and a W_d value in the range of > 440 to 480 kg/m^3 are denoted via a bold italic font; and (3) high MSR grade class grouping (2.0E to 2.4E) as defined as sawlog-sized trees having a M_e value in the range of > 13.5 to 16.5 GPa and a W_d value in the range of > 480 to 520 kg/m^3 are denoted via an italic font. Potentially problematic trees with M_a values greater that 15 are denoted by underlying where applicable.

slightly superior to those developed for jack pine, in terms the proportion of variation explained and overall predictive performance, the differences were of minor consequence.

The non-linear pattern of the jack pine developmental trajectories varied by attribute and systematically with cumulative size in respect to curve shape and rate of change (Fig. 5). The trends for the attributes most closely aligned with wood strength and stiffness, i.e., wood density, modulus of elasticity and cell wall thickness, could be characterized as polymorphic-like: values gradually increasing, attaining asymptotic maximums and thereafter gradually declining. The presence of directly proportional size-dependent effects suggested that the xylem tissue within larger-sized trees would be stronger and stiffer than that within smaller-sized trees (e.g.,W_d, M_e, $W_t \propto d_b$). The trends for microfibril angle indicated minimal size-dependent differentiation among the initial exponential-like declining trajectories that eventually stabilized over time. The attributes mostly aligned with pulp and paper performance metrics related to tear and tensile strength, i.e., fibre coarseness and specific surface area, differed in their size-dependence: directly proportional convex (C_o) versus inversely proportional (S_a) concave size-dependent polymorphic-like trends. The trajectories for tracheid diameters (radial and tangential) exhibited the most complex developmental patterns in terms of variable rates of change (e.g., rapid initial increases followed by temporal stability for D_r) and shifting size-dependence (e.g., from inversely to directly proportional within increasing cambial age for D_t).

Although the range of cambial age differed between species (maximum cambial ages of 41 and 71 for black spruce and jack pine, respectively), it is noteworthy that the size-dependent temporal trends observed for jack pine in this study differed from those reported for black spruce (Newton, 2016). For example, directly proportional size-dependent effects were found for all attributes but S_a for jack pine while inversely proportional size-dependence for W_d, M_e, W_t and directly proportional size-dependence for M_a, C_o, D_r, D_t and S_a were observed for black spruce. These species-specific differences imply that the solid-wood end-product potential increases with increasing tree size for jack pine and conversely decreases with increasing tree size for black spruce.

Table 6
Rotational stand-level and diameter-class densities and product volumes for jack pine and black spruce natural-origin stands and plantations situated on medium-to-good quality sites as predicted by the enhanced SSDMMs.

Stand-type[a]	Yield metric[b]	Unit	Stand-level	Diameter class level (cm)													
				2	4	6	8	10	12	14	16	18	20	22	24	26	28
$PNb_{(N)}$	Density	stems/ha	2950	6	111	336	566	671	591	389	278						
	Chip vol	m^3/ha	44					9	13	12	10						
	Lumber vol	m^3/ha	104					18	28	30	28						
$PNb_{(P)}$	Density	stems/ha	1370				4	21	67	149	253	323	296	179	77		
	Chip vol	m^3/ha	68						1	4	9	15	18	13	7		
	Lumber vol	m^3/ha	187						2	8	22	40	50	40	22		
$PIm_{(N)}$	Density	stems/ha	2782	3	49	167	333	488	559	507	362	315					
	Chip vol	m^3/ha	92					11	18	22	21	21					
	Lumber vol	m^3/ha	90					5	12	20	23	30					
$PIm_{(P)}$	Density	stems/ha	1383				1	4	14	38	87	164	253	309	278	167	69
	Chip vol	m^3/ha	122							1	4	10	19	28	29	20	9
	Lumber vol	m^3/ha	198							1	3	10	24	43	52	42	22

[a] As defined in Table 5.
[b] Chip vol and Lumber vol refer to recoverable chip and lumber volumes for a randomized-length sawmill processing protocol.

Although less definitive, the converse was true in regards to pulp and paper end-product potential: decreasing with increasing tree size for jack pine (exception being C_o) and increasing with increasing tree size for black spruce. These species-based differences may have important consequences for end-product potential for density manipulated stands where initial spacing or thinning treatments shifts the rotational diameter distribution towards the larger size classes.

4.2. Forecasting fibre attribute outcomes and assessing associated end-product potential

The integration of the new Silviscan-based Fibre Attributes submodule consisting of the suite of parameterized fibre attribute equations enabled the prediction of rotational estimates of wood density, microfibril angle, modulus of elasticity, fibre coarseness, tracheid wall thickness, tracheid radial diameter, tracheid tangential diameter and specific surface area by diameter class for a given density management regime and stand-type (e.g., Table 5). Although the resultant diameter class distribution of attribute estimates provides a fine-scale projection of wood quality characteristics for a given crop plan, the stand-level mean and associated measure of variation are also useful descriptive statistics for assessing overall differences and variability of end-product potentials among a set of competing crop plans. For example, comparing the stand-level mean values between the natural-origin and plantation stand-types for jack pine revealed that the plantation attributes were marginally superior although the magnitude of the differences was not overly disconcerting (Table 5). Conversely, the differences between the black spruce crop plans were consequential given that the stand-level attribute metrics for the plantation trees were considerably inferior to those for the trees within the natural-origin stand, particularly, for key solid-wood related attribute determinates (e.g., wood density, microfibril angle, and modulus of elasticity).

Design specifications for the 8 attributes examined in this study in terms of explicit linkages to end-product type (pulp and paper or solid wood products) and associated grade class have yet to be defined for standing trees. Consequently, explicit interpretation of attribute projections in terms of wood quality and associated end-product potential is problematic. However, contextual inferences can be extrapolated from (1) known end-product – attribute associations (Defo, 2008), (2) empirically from population-level sample-based comparisons, and (3) presumptively through direct application of grade rules. In relation to the first approach for example, increased quantity and quality of pulp and paper product yields would be conceptually associated with decreasing microfibril angle, and increasing fibre coarseness and specific surface area. Similarly, increased solid wood yields and grades would be conceptually associated with increasing wood density, modulus of elasticity and tracheid wall thickness (Bowyer et al., 2007).

With reference to the second approach, species-specific empirical-based population fibre attribute estimates derived from sample surveys of mature trees can provide a comparative range of values unique to a given species and region. For example, the selected jack pine crop plans considered in this study produced mean stand-level attribute values that were minimally inferior (≈10%) to their corresponding population-like sample means. Conversely, the results for the black spruce contrasts, particularly for the plantation crop plan, differences were much more dramatic (Table 5): e.g., declines of 21% in wood density and 32% in modulus of elasticity. Collectively, these differences could potentially translate into reduced lumber strength and stiffness of derived solid-wood end-products (dimensional lumber). Similarly, the higher microfibril angles and lower fibre coarseness, tracheid diameters, and specific surface areas associated with the black spruce plantation trees, could also result in reduced quantities and qualities of derived paper and paper related end-products. In regards to the third approach, presumptions can be used to infer solid-wood end-product potential using generalized grade-based attribute ranges provided in grading manuals for dimensional lumber products. For example, for the crop plans considered in this study, lumber end-product potential would varied considerably among diameter-classes. The grade of lumber produced from the sawlog-sized jack pine trees would systematically increase with increasing tree size irrespective of stand-type. Conversely, the grade of lumber extracted from sawlog-sized black spruce trees would systematically decline with increasing tree size. Collectively, as demonstrated in this study, all 3 indirect approaches can be of utility when attempting to interpret the SSDMM attribute predictions within the context of rotational end-product potential.

Although outside of the inference space of this study given the limited number of simulations examined, the rotational attribute forecasts for the black spruce plantation were nevertheless the most concerning in terms of the potential degrade in the quality of both end-product groups (solid-wood and pulp and paper products). This model-based result is not dissimilar to that reported for black spruce plantation experiments. Zhang et al. (2002) found that the wood quality attributes within trees from black spruce plantations were inferior to those trees grown in comparable natural-origin stands: specifically, plantation-grown black spruce lumber stiffness was 29% less than that of lumber produced from black spruce trees growing in stands which were of natural-origin. Although not directly comparable given differences in analytical approaches and subjective selection of the crop plans used for simulation, the experimental observations are coincidentally not dissimilar: mean stand-level modulus of elasticity of the plantation black spruce wood was on average, 33% less than that from the natural-origin stand at 50 years. Similar declines arising from stand structure

differences between stand-types can also be observed for the other attributes underlying end-product potential. For example, rotational plantation estimates of wood density, microfibril angle and fibre coarseness were inferior due principally to stand structure differences. Essentially, the reduction in intraspecific competition due to the lower initial establishment densities and the genetic worth effects resulted in accelerated rates of individual tree growth within the plantation which yielded consequential stand structural differences at rotation (e.g., increased number of larger-sized trees of reduced quality).

The hierarchical mixed-effects model specifications used for quantifying size-dependent fibre attribute developmental patterns in jack pine (this study) and black spruce (Newton, 2016), excluded consideration of stand-level effects given data limitations. Consequently, for a given species, the diameter-class mean attribute values are identical for overlapping classes irrespective of crop plan differences. Hence silvicultural treatment and stand origin effects on wood quality attributes are indirectly accounted for through stand structure differences. For example, the increased production of larger-sized black spruce trees of inferior quality for the plantation crop plan yielded an overall stand-level decline in wood quality: modulus of elasticity and wood density declined and microfibril angle increased. Furthermore, in terms of recoverable chip and lumber volumes, the plantations produced considerable greater product volumes than the natural-origin stand counterparts irrespective of species. Thus combined with the much greater lumber volumes being produced from plantations, potentially magnifies the wood quality differences to a consequential level in terms of the future wood supply. Black spruce wood quality concerns have also been raised from the results of initial spacing experiments where site occupancy levels have been manipulated. Specifically, Reid et al. (2009) reported that the relative distribution of MSR-rated lumber derived from two black spruce plantations established in northern Ontario on low quality sites (11.4 m at 30 years) differed according to stocking level. Specifically, 44, 51 and 3% of the dimensional lumber derived from the denser plantation (basal area of 41.1 m^2/ha at 45 years post-establishment) was classified as high (2100F-1.8E), medium (1650F-1.5E) and low (1450–1.3E) MSR grade classes, respectively. Conversely, no high or medium MRS grade class lumber products were produced from the plantation managed at the lower stocking level (basal area of 35.8 m^2/ha). Of further interest, Reid et al. (2009) also reported that visual grade assignments substantially over-estimated the higher grade percentages and under-estimated the lower grade percentages. Collectively, these results suggest that (1) caution should be exercised when considering establishing black spruce plantations at low densities when managing for lumber production, and (2) deploying modulus of elasticity estimates within the context of MSR-rating systems more precisely reflects the actual solid wood end-product potential than grade class estimates assigned through visual grading systems. These inferences and related experimental observations highlight the potential utility of the enhanced SSDMMs when managing for end-product potential. Specifically, via the provision of wood density and stiffness estimates which enable such MSR-like grade categorization along with estimates for other important fibre attributes associated with end-product type, grade and economic worth.

4.3. Modeling challenges and advancing value-based management decision-making

Modeling fibre attribute trajectories is a complex analytical endeavor given the competing age-dependent (ontogenetic) and growth-dependent (environmental) influences on fibre attribute formation. Diverse model-based approaches have been utilized in attempting to address this analytical challenge (e.g., Pokharel et al., 2014; Cortini et al., 2014; Wei et al., 2014; Townshend et al., 2015). However, most of the previous efforts have been focused on modelling a single attribute determinate of end-product potential at a single hierarchical level (e.g., temporal age-related developmental trends in wood density, microfibril angle or modulus of elasticity). Although this study developed models for describing the temporal developmental trajectories for a broader suite of attributes inclusive of secondary level effects (tree size), inclusion of population or stand-level effects are still lacking. The omission of incorporating these higher hierarchical sources of attribute variation in modeling studies is mostly due to the absence of large fibre attribute data bases that include Silviscan-equivalent attribute estimates obtained from the destructive sampling of a large number of trees within diverse stand structures at various stages of development across a species geographical range. This lack of stand-level driving variables such as stand density within the model specifications, negates the ability to account for initial spacing or thinning effects on attribute development within a given size class.

The enhanced SSDMMs developed in this study, does however, coarsely account for the overall effect these silvicultural treatments via the use of stand-level metrics that are reflective of treatment-induced changes in stand structure. As exemplified in the simulations, controlling initial spacing levels via plantation establishment and thus reducing inter-tree competition, can positively skew the rotational size class distributions. The resultant fibre attribute predictions yielded a set of wood quality performance metrics that can be used to inform density management decision-making. Nevertheless, in cases where responses to density management treatments do not appreciatively affect stand structure, treatment effects on attribute development patterns will be largely muted. Consequently, once the prerequisite fibre attribute data bases become available, development of tertiary-level hierarchical mixed-effects modeling specifications in which ring-level (cambial age; 1st level), tree-level (size; 2nd level) and stand-level (density and site qualilty; 3rd level) factors can be integrated, would be logical starting point for further research endeavors. Furthermore, the relative contribution of intrinsic genetic-driven versus environmental-driven effects on attribute variation is largely unknown for boreal conifers. The temporal developmental patterns of some attributes such as microfibril angle are considered to have a strong physiological-based underlying determinism (e.g., Lenz et al., 2010; Lachenbruch et al., 2011). Thus including tree-level and stand-level covariates for such attributes may yield limited gains in terms of increasing the portion of variation explained or enhancing the ability to delineate silvicultural treatment effects on rotational end-product potential outcomes.

Efforts to develop and integrate fibre attribute prediction equations within decision-support forecasting systems and silvicultural decision-support models is central to transitioning to a value-added product-based forest management paradigm (sensu Emmett, 2006a, 2006b). Globally, research initiatives in support of this aspiration goal have commence in various regions, resulting in the development of a number of decision-support models which can accommodate end-product considerations. These include the SILVA model built for Norway spruce (*Picea abies* (L.) Karst.) and other conifers and deciduous species in central Europe (Pretzsch et al., 2002), MOTTI model calibrated for Scots pine (*Pinus sylvestris* L.) and other conifers in Finland (Hynynen et al., 2005), FORSAT model parameterized for patula pine (*Pinus patula* (Schiede ex Schlect. & Cham.)) in South Africa (Kotze and Malan, 2007), and COFORD model developed for Sitka spruce (*Picea sitchensis* (Bong.) Carr.) in Great Britain (Gardiner et al., 2011). Apart from the SYLVER model developed for Douglas fir (*Pseudotsuga menziesii* (Mirb.) Franco) and other coniferous species in western Canada (Di Lucca, 1999), availability of similar decision-support models for other commercially-important species in Canada is limited (sensu Defo et al., 2016). The analytical approach and predictive scope of the enhanced SSDMMs presented in this study are not dissimilar to these next-generation decision-support tools. Although further modeling efforts in terms of explicitly accounting for the effects stand-level silviculture interventions (precommercial and commercial thinning) and site productivity differences on fibre attribute developmental trajectories may increase predictive precision in crop planning decision-making, the enhanced SSDMMs represent an incremental contribution towards value-based decision-making.

5. Conclusions

Successful transition from a volumetric yield maximization proposition to one based on maximizing product value within the Canadian forest sector is partially dependent on the provision of innovative tools that incorporate consideration of the principal determinates which underlie end-product potential (e.g., internal wood fibre attributes). For jack pine, an intensely-managed boreal species, this study developed, parameterized and evaluated a suite of hierarchical mixed-effects models for predicting the size-dependent temporal developmental trajectories for 8 fibre attributes explicitly related to end-product potential (wood density, microfibril angle, modulus of elasticity, fibre coarseness, tracheid wall thickness, tracheid radial diameter, tracheid tangential diameter and specific surface area). These jack pine equations along with those previously developed for black spruce, when integrated into the SSDMM structure, yielded an enhanced decision-support platform for evaluating fibre attribute outcomes and associated end-product consequences of competing crop plans. Collectively, these models represent an incremental advancement over traditional volumetric-based projection systems in that they can contribute to facilitating the paradigm shift towards value-based management for these commercially-important boreal species.

Acknowledgements

The author expresses his appreciation to: (1) Mike Laporte (Retired) of the Canadian Wood Fibre Centre, Canadian Forest Service (CFS), Natural Resources Canada (NRCan) and Gordon Brand of the Great Lakes Forestry Centre, CFS, NRCan, for field and laboratory data acquisition support; (2) Dr. Tessie Tong and Nelson Uy at FPInnovations, Vancouver, BC for completing the Silviscan-3 analysis, (3) the Canadian Wood Fibre Centre, CFS, NRCan for fiscal support, and (4) constructive comments and suggestions provided by the journal reviewers.

References

Barbour, R.J., Marshall, D.D., Lowell, E.C., 2003. Managing for wood quality. In: Monserud, R.A., Haynes, R.W., Johnson, A.C. (Eds.), Compatible Forest Management. Kluwer Academic Publishers, Netherlands, pp. 299–336.

Bowyer, J.L., Shmulsky, R., Haygreen, J.G., 2007. Forest Products and Wood Science: An Introduction, fifth ed. Blackwell Publishing, Ames, Iowa, USA.

Carmean, W.H., Hazenberg, G., Deschamps, K.C., 2006. Polymorphic site index curves for black spruce and trembling aspen in northwest Ontario. For. Chron. 82, 231–242.

Carmean, W.H., Niznowski, G.P., Hazenberg, G., 2001. Polymorphic site index curves for jack pine in Northern Ontario. For. Chron. 77, 141–150.

Cortini, F., Groot, A., Tong, Q., Duchesne, I., 2014. Ring-level models for predicting wood and fibre properties of *Abies balsamea*. Wood Sci. Technol. 48 (6), 1181–1196.

Daniel, C., Wood, F.S., 1980. Fitting Equations to Data, second ed. Wiley Inc., New York, NY, USA.

Defo, M., 2008. SilviScan-3—A Revolutionary Technology for High-Speed Wood Microstructure and Properties Analysis. Midis de al Foresterie; UQAT. Available online: http://chaireafd.uqat.ca/midiForesterie/pdf/20080422PresentationMauriceDefo.pdf (Assessed on 1 October 2018).

Defo, M., Duchesne, I., Stewart, J., 2016. A Review of the Current State of Wood Quality Modelling and Decision Support Systems in Canada. Natural Resources Canada, Canadian Forest Service, Information Report FI-X-012.

Di Lucca, C.M., 1999. TASS/SYLVER/TIPSY: systems for predicting the impact of silvicultural practices on yield, lumber value, economic return and other benefits. In: Barnsey, C. (Ed.), Proceedings of the Stand Density Management Planning and Implementation Conference; 1997 November 6-7; Edmonton, Alberta, Canada. Clear Lake Publishing Ltd., Edmonton, Alberta, Canada, pp. 7–16.

Ek, A.R., Monserud, R.A., 1979. Performance and comparison of stand growth models based on individual tree and diameter-class growth. Can. J. For. Res. 9, 231–244.

Emmett, B., 2006a. Increasing the value of our forest. For. Chron. 82, 3–4.

Emmett, B., 2006b. Perspectives on sustainable development and sustainability in the Canadian forest sector. For. Chron. 82, 40–43.

Evans, R., 1994. Rapid measurement of the transverse dimensions of tracheids in radial wood sections from *Pinus radiata*. Holzforschung 48, 168–172.

Evans, R., 2006. Wood stiffness by X-ray diffractometry. In: Stokke, D.D., Groom, L.H. (Eds.), Characterization of the Cellulosic Cell Wall. Wiley, Hoboken, NJ, USA, pp. 138–146.

Evans, R., Stuart, S.A., Van Der Touw, J., 1996. Microfibril angle scanning of increment cores by X-ray diffractometry. Appita J. 49, 411–414.

Gardiner, B., Leban, J.-M., Auty, D., Simpson, H., 2011. Models for predicting wood density of British-grown Sitka spruce. Forestry 84, 119–132.

Gribko, L.S., Wiant Jr., H.V., 1992. A SAS template program for the accuracy test. Compiler 10, 48–51.

Gujarati, D.N., 2006. Essential of Econometrics, third ed. McGraw-Hill, New York, NY, USA.

Hoerl, A.E., 1954. Fitting curves to data. In: Perry, J.H. (Ed.), Chemical Business Handbook. McGraw-Hill, New York, NY, USA, pp. 55–77.

Hynynen, J., Ahtikoski, A., Siitonen, J., Sievanen, R., Liski, J., 2005. Applying the MOTTI simulator to analyse the effects of alternative management schedules on timber and non-timber production. For. Ecol. Manage. 207, 5–18.

Kang, K.-Y., Zhang, S.Y., Mansfield, S.D., 2004. The effects of initial spacing on wood density, fibre and pulp properties in jack pine (*Pinus banksiana* Lamb.). Holzforschung 58, 455–463.

Kira, T., Ogawa, H., Sakazaki, N., 1953. Intraspecific competition among higher plants. I. Competition-yield-density interrelationship in regularly dispersed populations. J. Inst. Polytech. (Osaka City Univ., Japan) Series D 4, 1–16.

Kotze, H., Malan, F., 2007. Further progress in the development of prediction models for growth and wood quality of plantation-grown Pinus patula sawtimber in South Africa. In: Dykstra, D.P., Monserud, R.A. (Eds.), Proceedings of the Forest Growth and Timber Quality: Crown Models and Simulation Methods for Sustainable Forest Management Conference; 2007, August 7-10; Portland, Oregon, USA, General Technical Report, PNW-GTR-791, Department of Agriculture, Forest Service, Pacific Northwest Research Station, Portland, OR, pp. 113–123.

Lachenbruch, B., Moore, J., Evans, R., 2011. Radial variation in wood structure and function in woody plants, and hypotheses for its occurrence. In: Meinzer, C., Lachenbruch, B., Dawson, T.E. (Eds.), Size- and Age-related Changes in Tree Structure and Function. Springer, Netherlands, pp. 121–164.

Lenz, L., Cloutier, A., MacKay, J., Beaulieu, J., 2010. Genetic control of wood properties in *Picea glauca* - an analysis of trends with cambial age. Can. J. For. Res. 40, 703–715.

McKinnon, L.M., Kayahara, G.J., White, R.G., 2006. Biological framework for commercial thinning even-aged single-species stands of jack pine, white spruce, and black spruce in Ontario [online]. Available at http://www.forestresearch.ca/images/stories/pdf/tr-046.pdf (Accessed 20/10/2018).

National Lumber Grades Authority (NLGA), 2013. Special Products Standard for Machine Graded Lumber. NLGA, Surrey, BC, Canada.

Neter, J., Wasserman, W., Kutner, M.H., 1990. Applied Linear Statistical Models, third ed. Irwin, Boston, MA, USA.

Newton, P.F., 2003. Systematic review of yield responses of four North American conifers to forest tree improvement practices. For. Ecol. Manage. 172, 29–51.

Newton, P.F., 2006. Asymptotic size–density relationships within self-thinning black spruce and jack pine stand-types: Parameter estimation and model reformulations. For. Ecol. Manage. 226, 49–59.

Newton, P.F., 2009. Development of an integrated decision-support model for density management within jack pine stand-types. Ecol. Model. 220, 3301–3324.

Newton, P.F., 2012a. A decision-support system for density management within upland black spruce stand-types. Environ. Modell. Software 35, 171–187.

Newton, P.F., 2012b. A silvicultural decision-support algorithm for density regulation within peatland black spruce stands. Comput. Electron. Agric. 80, 115–125 + Supplementary Online Material.

Newton, P.F., 2012c. Development and utility of an ecological-based decision-support system for managing mixed coniferous forest stands for multiple objectives (ISBN: 978-1-61324-567-5) In: Zhang, W. (Ed.), Ecological Modeling, Environmental Science, Engineering and Technology Book Series. Nova Scientific Publishers, pp. 115–172.

Newton, P.F., 2015a. Genetic worth effect models for boreal conifers and their utility when integrated into density management decision-support systems. Open J. Forestry 5, 105–115.

Newton, P.F., 2015b. Quantifying growth responses of black spruce and jack pine to thinning within the context of density management decision-support systems. Open J. Forestry 5, 409–421.

Newton, P.F., 2015c. Evaluating the ecological integrity of structural stand density management models developed for boreal conifers. Forests 6, 992–1030.

Newton, P.F., 2016. Quantifying size-dependent developmental trajectories of commercial-relevant fibre attributes within maturing black spruce plantations employing hierarchical linear models. For. Ecol. Manage. 381, 1–16.

Newton, P.F., Amponsah, I.G., 2005. Evaluation of Weibull-based parameter prediction equation systems for black spruce and jack pine stand types within the context of developing structural stand density management diagrams. Can. J. For. Res. 35, 2996–3010.

Newton, P.F., Amponsah, I.G., 2007. Comparative evaluation of five height–diameter models developed for black spruce and jack pine stand-types in terms of goodness-of-fit, lack-of-fit and predictive ability. For. Ecol. Manage. 247, 149–166.

Pokharel, B., Dech, J.P., Groot, A., Pitt, D., 2014. Ecosite-based predictive modeling of black spruce (*Picea mariana*) wood quality attributes in boreal Ontario. Can. J. For. Res. 44 (5), 465–475.

Porté, A., Barlelink, H.H., 2002. Modelling mixed forest growth: a review of models for forest management. Ecol. Model. 150, 141–188.

Pretzsch, H., Biber, P., Dursky, J., 2002. The single tree-based stand simulator SILVA: construction, application and evaluation. For. Ecol. Manage. 162, 3–21.

Rais, A., Poschenrieder, W., Pretzsch, H., van de Kuilen, J.G., 2014. Influence of initial plant density on sawn timber properties for Douglas-fir (*Pseudotsuga menziesii* (Mirb.) Franco). Ann. Forest Sci. 71, 617–626.

Ratkowsky, D.A., 1990. Handbook of Nonlinear Regression Models. Marcel Dekker, New York, NY, USA.

Raudenbush, S.W., Bryk, A.S., 2002. Hierarchical Linear Models: Applications and Data Analysis Methods, second ed. Sage, Newbury Park, CA, USA.

Raudenbush, S.W., Bryk, A.S., Cheong, Y.F., Congdon Jr., R.T., du Toit, M., 2011. HLM 7 –

Hierarchical Linear and Nonlinear Modeling. Scientific Software International Inc., Lincolnwood, IL, USA.
Reid, D.E.B., Young, S., Tong, Q., Zhang, S.Y., Morris, D.M., 2009. Lumber grade yield, and value of plantation-grown black spruce from 3 stands in northwestern Ontario. For. Chron. 85 (4), 609–617.
Reynolds Jr., M.R., 1984. Estimating the error in model predictions. Forest Sci. 30, 454–469.
Rowe, J.S., 1972. Forest regions of Canada. Government of Canada, Department of Environment, Canadian Forestry Service, Ottawa, Ontario. Publication No. 1300.
Shinozaki, K., Kira, T., 1956. Intraspecific competition among higher plants. VII. Logistic theory of the C-D effect. J. Inst. Polytech. (Osaka City Univ., Japan), Ser. D 12, 69–82.
Sprugel, D.G., 1983. Correcting for bias in log-transformed allometric equations. Ecology 64, 209–210.
Townshend, E., Pokharel, B., Groot, A., Pitt, D., Dech, J.P., 2015. Modeling wood fibre length in black spruce (*Picea mariana* (Mill.) B.S.P.) based on ecological land classification. Forests 2015 (10), 3369–3394.
Watt, M.S., Zoric, B., Kimberley, M.O., Harrington, J., 2011. Influence of stocking on radial and longitudinal variation in modulus of elasticity, microfibril angle, and density in a 24-year-old *Pinus radiata* thinning trial. Can. J. For. Res. 41, 1422–1431.
Wei, X., Leitch, M., Auty, D., Duchateau, E., Achim, A., 2014. Radial trends in black spruce wood density can show an age- and growth-related decline. Ann. Forest Sci. 71 (5), 603–615.
Yoda, K., Kira, T., Ogawa, H., Hozumi, K., 1963. Self-thinning in overcrowded pure stands under cultivated and natural-origin conditions. J. Biol. (Osaka City Univ., Japan) 14, 107–129.
Zhang, S.Y., Chauret, G., Ren, H.Q., Desjardins, R., 2002. Impact of plantation black spruce initial spacing on lumber grade yield, bending properties and MSR yield. Wood Fibre Sci. 34, 460–475.
Zhang, S.Y., Koubaa, A., 2008. Softwoods of eastern Canada: their silvics, characteristics, manufacturing and end-uses. Special Publication SP-526E, FPInnovations, St. Foy, Quebec City, Quebec, Canada.